



# **NAVAL POSTGRADUATE SCHOOL**

**MONTEREY, CALIFORNIA**

## **THESIS**

**NEAR FIELD IMAGING OF GALLIUM NITRIDE  
NANOWIRES FOR CHARACTERIZATION OF MINORITY  
CARRIER DIFFUSION**

by

Lee G. Baird

December 2009

Thesis Advisor:  
Second Reader:

Nancy M. Haegel  
James Luscombe

**Approved for public release; distribution is unlimited**

<b>REPORT DOCUMENTATION PAGE</b>			<i>Form Approved OMB No. 0704-0188</i>	
Public reporting burden for this collection of information is estimated to average 1 hour per response, including the time for reviewing instruction, searching existing data sources, gathering and maintaining the data needed, and completing and reviewing the collection of information. Send comments regarding this burden estimate or any other aspect of this collection of information, including suggestions for reducing this burden, to Washington headquarters Services, Directorate for Information Operations and Reports, 1215 Jefferson Davis Highway, Suite 1204, Arlington, VA 22202-4302, and to the Office of Management and Budget, Paperwork Reduction Project (0704-0188) Washington DC 20503.				
<b>1. AGENCY USE ONLY (Leave blank)</b>		<b>2. REPORT DATE</b> December 2009	<b>3. REPORT TYPE AND DATES COVERED</b> Master's Thesis	
<b>4. TITLE AND SUBTITLE</b> Near Field Imaging of Gallium Nitride Nanowires for Characterization of Minority Carrier Diffusion.			<b>5. FUNDING NUMBERS</b>	
<b>6. AUTHOR(S)</b> Lee G. Baird				
<b>7. PERFORMING ORGANIZATION NAME(S) AND ADDRESS(ES)</b> Naval Postgraduate School Monterey, CA 93943-5000			<b>8. PERFORMING ORGANIZATION REPORT NUMBER</b>	
<b>9. SPONSORING /MONITORING AGENCY NAME(S) AND ADDRESS(ES)</b> N/A			<b>10. SPONSORING/MONITORING AGENCY REPORT NUMBER</b>	
<b>11. SUPPLEMENTARY NOTES</b> The views expressed in this thesis are those of the author and do not reflect the official policy or position of the Department of Defense or the U.S. Government.				
<b>12a. DISTRIBUTION / AVAILABILITY STATEMENT</b> Approved for public release; distribution is unlimited			<b>12b. DISTRIBUTION CODE</b>	
<b>13. ABSTRACT (maximum 200 words)</b> A novel system has been developed for the imaging of carrier transport within semiconductor nanostructures by operating a near field scanning optical microscopy (NSOM) within a scanning electron microscope. Luminescence associated with carrier recombination is collected with high spatial resolution to monitor the motion and recombination of charge generated by use of an electron beam as an independent point source. Light is collected in the near field from a scanning fiber using tuning fork feedback in an open architecture combined AFM/NSOM system allowing for independent motion of sample and tip. From a single image, it is possible to obtain a direct measure of minority carrier diffusion length. This technique has been used in the near-field collection mode to image the diffusion of holes in n-type GaN-AlGaIn core-shell nanowires, unintentionally doped GaN nanowires and p-type GaN nanowires grown via Ni-catalyzed MOCVD. Measurements were made on tapered nanowires ranging in diameter from 500 to 800 nm, with lengths up to ~ 30 µm. The average 1-dimensional carrier diffusion length was measured to be 1.3 +/- 0.2 µm for GaN/AlGaIn core-shell, 0.96 +/- 0.25 µm for the uncoated GaN wires, and 0.65 +/- 0.35 µm for the p-type uncoated GaN wires in the low injection limit.				
<b>14. SUBJECT TERMS</b> Transport imaging, Minority carrier, GaN nanowires, Diffusion length, Near-field scanning optical microscopy, NSOM			<b>15. NUMBER OF PAGES</b> 83	
			<b>16. PRICE CODE</b>	
<b>17. SECURITY CLASSIFICATION OF REPORT</b> Unclassified	<b>18. SECURITY CLASSIFICATION OF THIS PAGE</b> Unclassified	<b>19. SECURITY CLASSIFICATION OF ABSTRACT</b> Unclassified	<b>20. LIMITATION OF ABSTRACT</b> UU	

THIS PAGE INTENTIONALLY LEFT BLANK

**Approved for public release; distribution is unlimited**

**NEAR FIELD IMAGING OF GALLIUM NITRIDE NANOWIRES FOR  
CHARACTERIZATION OF MINORITY CARRIER DIFFUSION**

Lee G. Baird  
Lieutenant Commander, United States Navy  
B.S., United States Naval Academy, 1994

Submitted in partial fulfillment of the  
requirements for the degree of

**MASTER OF SCIENCE IN APPLIED PHYSICS**

from the

**NAVAL POSTGRADUATE SCHOOL  
December 2009**

Author: Lee G. Baird

Approved by: Nancy M. Haegel  
Thesis Advisor

James Luscombe  
Second Reader

Andres Larraza  
Chairman, Department of Physics

THIS PAGE INTENTIONALLY LEFT BLANK

## ABSTRACT

A novel system has been developed for the imaging of carrier transport within semiconductor nanostructures by operating a near field scanning optical microscopy (NSOM) within a scanning electron microscope. Luminescence associated with carrier recombination is collected with high spatial resolution to monitor the motion and recombination of charge generated by use of an electron beam as an independent point source. Light is collected in the near field from a scanning fiber using tuning fork feedback in an open architecture combined AFM/NSOM system allowing for independent motion of sample and tip. From a single image, it is possible to obtain a direct measure of minority carrier diffusion length. This technique has been used in the near-field collection mode to image the diffusion of holes in n-type GaN-AlGaIn core-shell nanowires, unintentionally doped GaN nanowires and p-type GaN nanowires grown via Ni-catalyzed MOCVD. Measurements were made on tapered nanowires ranging in diameter from 500 to 800 nm, with lengths up to  $\sim 30 \mu\text{m}$ . The average 1-dimensional carrier diffusion length was measured to be  $1.3 \pm 0.2 \mu\text{m}$  for GaN/AlGaIn core-shell,  $0.96 \pm 0.25 \mu\text{m}$  for the uncoated GaN wires, and  $0.65 \pm 0.35 \mu\text{m}$  for the p-type uncoated GaN nanowires in the low injection limit.

THIS PAGE INTENTIONALLY LEFT BLANK

## TABLE OF CONTENTS

<b>I.</b>	<b>INTRODUCTION.....</b>	<b>1</b>
<b>A.</b>	<b>BACKGROUND .....</b>	<b>1</b>
<b>II.</b>	<b>TRANSPORT IMAGING .....</b>	<b>5</b>
<b>A.</b>	<b>SEMICONDUCTOR BASICS.....</b>	<b>5</b>
<b>B.</b>	<b>CATHODOLUMINESCENCE (CL).....</b>	<b>7</b>
<b>C.</b>	<b>IMAGING CHARGE TRANSPORT .....</b>	<b>8</b>
<b>D.</b>	<b>NEAR FIELD SCANNING OPTICAL MICROSCOPY (NSOM).....</b>	<b>10</b>
<b>E.</b>	<b>ATOMIC FORCE MICROSCOPY (AFM) .....</b>	<b>12</b>
<b>III.</b>	<b>EXPERIMENTAL SETUP .....</b>	<b>15</b>
<b>A.</b>	<b>EQUIPMENT USED .....</b>	<b>15</b>
<b>1.</b>	<b>Scanning Electron Microscope (SEM) .....</b>	<b>15</b>
<b>a.</b>	<i>Picture Mode .....</i>	<i>16</i>
<b>b.</b>	<i>Line Mode.....</i>	<i>16</i>
<b>c.</b>	<i>Spot Mode.....</i>	<i>16</i>
<b>2.</b>	<b>AFM/NSOM .....</b>	<b>16</b>
<b>a.</b>	<i>AFM Scanning Probe is an NSOM Fiber .....</i>	<i>17</i>
<b>b.</b>	<i>Optical Access to the Sample .....</i>	<i>17</i>
<b>c.</b>	<i>Independent Scanning Plates .....</i>	<i>18</i>
<b>d.</b>	<i>MultiView 2000 Specifications .....</i>	<i>20</i>
<b>B.</b>	<b>EXPERIMENTAL APPROACH .....</b>	<b>21</b>
<b>1.</b>	<b>Considerations.....</b>	<b>22</b>
<b>a.</b>	<i>Grounding of the Sample.....</i>	<i>22</i>
<b>b.</b>	<i>Grounding of the NSOM Tip.....</i>	<i>22</i>
<b>c.</b>	<i>Interactions between the NSOM Tip and the Nanowire .....</i>	<i>25</i>
<b>IV.</b>	<b>MATERIALS .....</b>	<b>29</b>
<b>A.</b>	<b>GALLIUM NITRIDE.....</b>	<b>29</b>
<b>1.</b>	<b>Growth Details .....</b>	<b>29</b>
<b>2.</b>	<b>GaN Nanowire Characteristics.....</b>	<b>30</b>
<b>V.</b>	<b>EXPERIMENTAL RESULTS.....</b>	<b>33</b>
<b>A.</b>	<b>GAN/ALGAN CORE-SHELL NANOWIRES.....</b>	<b>33</b>
<b>B.</b>	<b>UNCOATED GALLIUM NITRIDE NANOWIRES .....</b>	<b>39</b>
<b>1.</b>	<b>Unintentionally Doped (UID) GaN Nanowires.....</b>	<b>39</b>
<b>C.</b>	<b>MAGNESIUM DOPED (P-TYPE) GAN NANOWIRES.....</b>	<b>41</b>
<b>VI.</b>	<b>CONCLUSIONS AND SUGGESTIONS FOR FURTHER RESEARCH.....</b>	<b>45</b>
<b>A.</b>	<b>CONCLUSIONS .....</b>	<b>45</b>
<b>B.</b>	<b>SUGGESTIONS FOR FURTHER RESEARCH.....</b>	<b>46</b>
<b>1.</b>	<b>Study of GaN Nanowire Waveguide Modes .....</b>	<b>46</b>
<b>2.</b>	<b>Transport Imaging of Charge with an Applied Electric Field .....</b>	<b>46</b>
<b>3.</b>	<b>Further Investigation on Diffusion Lengths in Other Materials...46</b>	



4. Optimization of Probe Tips to Limit Charge and Drifting Effects.....	47
APPENDIX A. ARTICLE ON TRANSPORT IMAGING [15] .....	49
APPENDIX B. ARTICLE ON GALLIUM NITRIDE NANOWIRE DIFFUSION LENGTH WITH NSOM [24] .....	59
LIST OF REFERENCES .....	63
INITIAL DISTRIBUTION LIST .....	65

## LIST OF FIGURES

Figure 1.	Energy Band Diagram for GaN. From [7].....	5
Figure 2.	CL Spectrum of GaN Nanowire. From [9]. ....	7
Figure 3.	Minority carrier diffusion in (a) InGaP (b) GaAs (c) InGaAs with (d) semilog plot showing calculated diffusion lengths. From [11].....	9
Figure 4.	Optical picture of two 10 micron GaN nanowires with CCD camera. ....	10
Figure 5.	Definition of Far and Near field optics. From [9].....	11
Figure 6.	SEM picture of an NSOM tip. ....	12
Figure 7.	Forces acting on an AFM tip. From [14] .....	13
Figure 8.	Schematic Diagram of the AFM/NSOM probe. From [9].....	17
Figure 9.	Top (a) and Reverse (b) Views of the AFM/NSOM Probe Attached onto the MultiView 2000 Scanner. ....	18
Figure 10.	Nanonics MultiView 2000 Scanner in the JEOL 840 SEM. ....	19
Figure 11.	(a) Counterclockwise from Top Left Corner: Low Voltage Adapter, HVPD for Upper Stage, SPM Controller, HVPD for Lower Stage and Counter and Power Supply for the APD. (b) The APD for Detecting Photons from the Fiber Probe During Measurements.....	21
Figure 12.	NSOM Scan with an Externally Excited Generation Source. From [9] .....	22
Figure 13.	SEM pictures (a) demonstrating NSOM glue charging and distorting picture and (b) showing minimal distortion.....	23
Figure 14.	NSOM picture captured using 'spot' mode. ....	24
Figure 15.	(a) Raw and (b) corrected NSOM data captured in 'pic' mode. ....	25
Figure 16.	Dimension of a typical nanowire and the NSOM tip.....	26
Figure 17.	Illustration of MOCVD process. From [3] .....	30
Figure 18.	Growth process for a nanowire in the quartz tube furnace. From [22].....	30
Figure 19.	(a) and (b) are SEM picture of GaN nanowire showing the length and cross section characteristics. From [21].....	31
Figure 20.	Topography (a), near-field luminescence and (b) image from a GaN nanowire under point source excitation. The image dimensions are 10 $\mu\text{m}$ x 10 $\mu\text{m}$ . ....	34
Figure 21.	3-D combination of topography and near-field luminescence from a GaN nanowire under point source excitation. ....	35
Figure 22.	(a) Depicts how a nanowire will waveguide light and (b) show NSOM intensity data on a GaN nanowire with SEM excitation point in the middle and evidence of waveguiding at both ends. ....	36
Figure 23.	Intensity as a function of distance resulting from minority carrier in 1D resulting in minority carrier profiles. GaN wire diameter is 500 nm. Excitation conditions were 20 keV and $3 \times 10^{-10}$ A probe current in line mode.....	37
Figure 24.	Intensities as a function of distance. GaN wire diameter is 700 nm. Excitation conditions were 20keV and different probe currents ( $6 \times 10^{-12}$ , $3 \times 10^{-11}$ , $1 \times 10^{-10}$ , and $6 \times 10^{-10}$ A).....	38

Figure 25.	Intensity as a function of distance resulting from minority carrier in 1D resulting in minority carrier diffusion profile. UID GaN wire diameter is 600 nm. Excitation conditions were 20 keV and $1 \times 10^{-10}$ A probe current in line mode.....	40
Figure 26.	NSOM Intensity as a function of distance of two UID GaN wire with diameters 600 nm each. Excitation conditions were 20keV and different probe currents ( $3 \times 10^{-10}$ , and $1 \times 10^{-10}$ A). .....	41
Figure 27.	NSOM Intensity as a function of distance of a P-type GaN wire with diameter is 800 nm. Excitation conditions were 20 keV and $6 \times 10^{-10}$ A probe current in line mode. ....	42
Figure 28.	Intensities as a function of distance on three types of scans on the same p-type GaN wire. Wire diameter was 600 nm. Excitation conditions were 20 keV and $6 \times 10^{-10}$ A probe current with different SEM modes (Spot, Picture, and Line). ....	43

## LIST OF TABLES

Table 1.	30 keV SEM beam with width diameter dependence on probe current. From [16] .....	15
Table 2.	MultiView 2000 specifications. From [17].....	20
Table 3.	AFM settings to optimize contact between NSOM tip and nanowire .....	26
Table 4.	Results for GaN diffusion lengths.....	45

THIS PAGE INTENTIONALLY LEFT BLANK

## **LIST OF ACRONYMS AND ABBREVIATIONS**

AFM	Atomic Force Microscopy
CCD	Charged-Couple Device
CL	Cathodal Luminescence
DARPA	Defense Advanced Research Project Agency
EBIC	Electron Beam Induced Current
GaN	Gallium Nitride
LED	Light Emitting Diode
MOCVD	Metal-Organic Chemical Vapor Deposition
NSOM	Near-Field Scanning Optical Microscopy
SEM	Scanning Electron Microscopy
TRPL	Time Resolved Photo Luminescence
VLS	Vapor-Liquid-Solid
UID	Unintentionally Doped

THIS PAGE INTENTIONALLY LEFT BLANK

## ACKNOWLEDGMENTS

First acknowledgement goes out to my loving wife, Yibeli Galindo-Baird, for providing me the love, support, proofreading services, and the time to complete my research/thesis writing. She has always inspired me to go for the brass ring and leave nothing to chance. If it were not for her, I would not be where I am today. Thank you!

Second acknowledgement goes out to my outstanding thesis advisor, Dr. Nancy Haegel. She was more than a thesis advisor, she was a mentor. Constantly providing feedback, I was able to stay the course, produce this thesis, and publish an article in a journal before I graduated from NPS. Her leadership and tenacity helped me become not only a better master's student, but a better person. I am fully grateful for all that she has taught me.

My appreciation extends to Dr. A. Alec Talin and Dr. George Wang of Sandia National Laboratories for the GaN nanowires. Hesham Taha with Nanonics for showing me the in-and-outs of the MultiView 2000 and former thesis student Chung Hong Low for teaching me his tricks on how to use the MultiView 2000.

This work was supported by National Science Foundation Grants DMR 0526330 and 0804527. The budget was sufficient for me to experiment without fear of running out of money. AFM/NSOM data collection is a contact sport and healthy funding ensures plenty of nanowires and AFM/NSOM tips.

To my fellow classmates of the Physics Department graduating class of December 2009: It was great having the whole bunch together. We were a very tight team and we got through a lot together.

Last but not least, my parents, Maria and John Baird, for raising me the right way!



THIS PAGE INTENTIONALLY LEFT BLANK

# **I. INTRODUCTION**

## **A. BACKGROUND**

Semiconductors have been at the center of almost every technological advance in the past 40 years. Cell phones, personal computers, and digital cameras are all prime examples of how society has benefited tremendously from these advances. However, our technological society is also continuously trying to make these items more practical, efficient, and portable. To achieve these goals, scientist and engineers need to fabricate semiconductor structures that are smaller and smaller. To continue to shrink these devices, the semiconductor materials that make up these structures are starting to approach a size at which Newtonian mechanics no longer apply to the behavior of the electrons and holes that carry charge. Additionally, the effects of quantum mechanical phenomena need to be considered.

In 1947, the first transistor was created at the AT&T Bell labs. It was made out of germanium and was almost half a meter long [1]. Now, transistors are etched into silicon wafers at the size of a micron [2], giving the modern personal computer the memory and processing power it has today. The next anticipated technological leap is using semiconductor nanowires to design the next generation of devices. These last few years, nanowires have been demonstrated to be usable for communications, spectroscopic sensing, computational technology, solar/alternative energy, and the biological sciences, by taking advantage of their unique thermal, optoelectronic, chemical, and mechanical properties [3].

Nanowires are defined as semiconductor wires with a diameter on the order of nanometers. At that scale, material properties do not behave as bulk materials, but as one-dimensional materials. The electrons in these structures may be quantum confined and the surface will play a major role. The fundamental behavior of semiconductor nanowires needs to be studied for possible future applications, in the same way that earlier bulk and thin film materials were extensively characterized.

Scientific research facilities and industries have been creating nanowires since the early 1960s with a vapor-liquid-solid (VLS) growth technique [3]. By applying epitaxial crystal growth techniques to the VLS process, growth orientation can be obtained. However, this process is not ideal for industrial mass production. Metal-organic chemical vapor deposition (MOCVD) has shown promise for mass production without losing the growth direction control.

As the nanowire community has developed new and improved ways to grow these nano-structures, new characterization tools must also be developed that are commensurate with the scale of these new materials. These methods need to be quick and easy to use and at the same time, provide accurate results.

This research is particularly interested in developing a novel approach to measure the minority carrier diffusion length in nanowires. Understanding the minority carrier diffusion length in nanowires is critical to potential applications in solar cells, spectroscopic sensing, and/or lasers and light emitting diodes (LED). Traditionally, determining the diffusion lengths of these nanowires was an involved process that required having a nanowire contacted with two electrical leads and exciting the wire with either a laser or an electron beam from an electron microscope. This process was time consuming and did not provide a high degree of flexibility or spatial resolution. New methods are needed to accurately determine the diffusion length in these novel structures.

This thesis focuses on a unique optical way to measure diffusion length that is being pioneered at the Naval Postgraduate School. This process is an easier, more accurate, and less time-consuming approach than traditional electrical methods. By using the optical properties of semiconductors, the diffusion length can be determined by exciting minority carriers and observing the photons that are emitted when they recombine. This technique has been successfully demonstrated with thin film solar cell materials [4, 5]. In these experiments, the diffusion length was measured using a Silicon charged couple device (CCD) camera. The light intensity was captured by the camera in the far field, and the spatial information was observed and analyzed.

However, this technique cannot be used for nanowires since both the structures of interest and the diffusion lengths may be too small for the resolution of the far-field optics. Near-Field Scanning Optical Microscopy (NSOM) has to be used to collect the emitted light with sufficient spatial resolution to correctly determine the diffusion length. This NSOM capability is coupled with an Atomic Force Microscopy (AFM) to provide both the spatial and light intensity mapping to determine accurate minority carrier diffusion lengths.

## **B. MILITARY RELEVANCE**

Nano-technology has shown a tremendous amount of promise from reducing the size of sensors and miniaturizing lasers, to shrinking the super computer down to the size of a thumb nail. The military is continually looking to reduce weight, power and size restrictions. With the maturing of nano-technology, the Department of Defense will be able to realize these goals.

It is hard to predict the possible use of a technology that is not fully understood. As the understanding of these properties emerge, it may take scientists and engineers down a separate path and a completely different set of applications, which could solve a much different set of problems from what is projected today. For example, the Defense Advanced Research Projects Agency (DARPA) is looking into infra-red sensors that consist of cooled semiconductors, namely bismuth telluride. If the sensor consisted of bismuth telluride nanowires, the amount of cooling required would be reduced from a bulk cooling system to a micro-cooler using only 0.1 Watts reducing the temperature to -200°C [6]. Other projects on which DARPA has been working are: the atomic clock on a chip, radar on a chip, gas analyzers, radio frequency, and photonic devices. This work is still ongoing, but the results look promising.

Thus, experiments, measurements, and analysis are needed to ensure these nanostructures are understood and can be fully exploited by our military. The basic science investment leads to direct military impact as seen historically in the development of lasers, information processing and detectors.

THIS PAGE INTENTIONALLY LEFT BLANK

## II. TRANSPORT IMAGING

### A. SEMICONDUCTOR BASICS

The existence of an energy band gap in semiconductor materials is what makes them useful in electronics. Semiconductor electron energy states can be defined in two bands of energy: a valence band and a conduction band. When the semiconductor is in its lowest energy state, the electrons exist in the valence band, which does not allow the electrons to move freely, therefore not allowing a net current to flow. When energy is applied to the semiconductor, whether it be from heat or photons or electrons that have enough energy to overcome the band gap, electrons in the valence band transition to the conduction band where they are free to conduct current. When the electron moves to the conduction band, a positive hole is created due to the absence of an electron in the valence band. This hole is also free to move and can contribute to current flow. Figure 1 shows the energy band diagram for Gallium Nitride (GaN) where the band gap energy required to move an electron from the valence band to the conduction band at room temperature is 3.4 eVs [7].

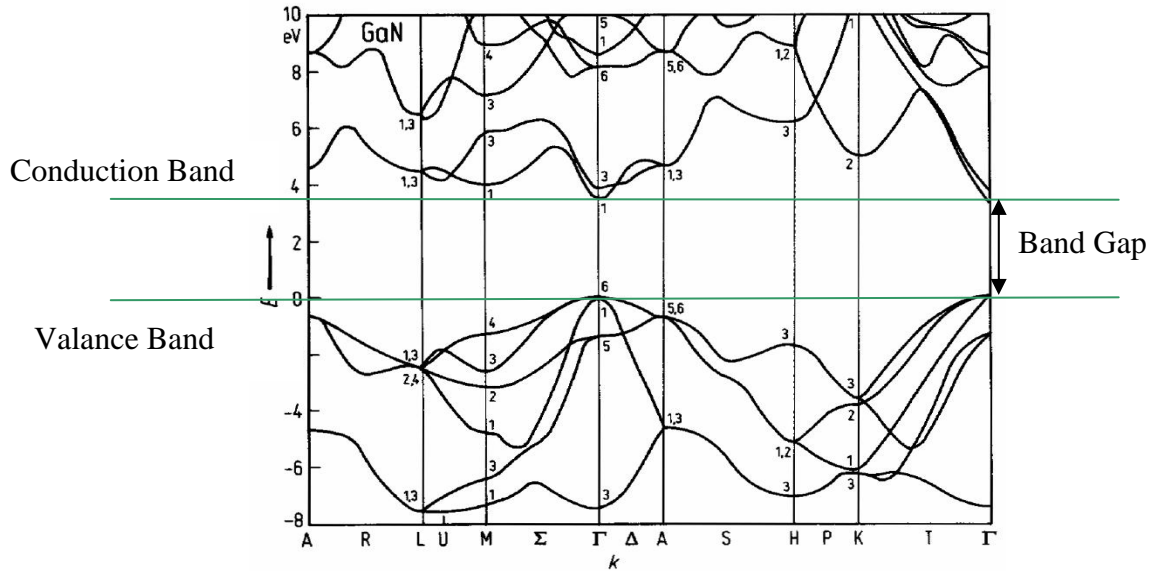


Figure 1. Energy Band Diagram for GaN. From [7]

An electron that has been excited into the conduction band has a limited lifetime and has to recombine with a positive hole in the valence band. This lifetime is different for each semiconductor material. It is a key parameter, however, especially for devices such as lasers and bipolar transistors that depend on the behavior of non-equilibrium carriers. Time resolved photoluminescence (TRPL) measurements of lifetime in GaN nanowires have ranged from 200 ps to over 2 ns [8]. The large range is attributed to variance in diameter, dopant levels and temperature of the semiconductor.

To understand how well a semiconductor will conduct electricity, its lifetime must be known as well as how easily an electron/positive hole can move in its respective band. The combination of the lifetime and the mobility of charge will define a diffusion length as:

$$L_d = \sqrt{\frac{kT}{e}} \mu \tau$$

where  $L_d$  is the diffusion length,  $k$  is Boltzmann's constant,  $T$  is the temperature in Kelvin,  $\mu$  is the charge carrier mobility and  $\tau$  is the minority charge carrier lifetime.

All semiconductors will have doping, meaning the material will have an excess of either electrons in the valance band or positive holes in the conduction band due to defects in the growth process or intentional addition of elements by the growers. The majority carrier is charge (electrons or holes) that is in abundance. The minority carrier is the charge carrier that does not have excess charge. For example, in an n-type doped semiconductor, the majority carriers are the electrons because there are abundant free electrons in the valence band and the minority carriers are the holes; holes are only created when excited by an outside influence and electron-hole pairs are created. The light collected in these experiments reflects the minority carrier recombination.

## B. CATHODOLUMINESCENCE (CL)

After the average life, it will recombine with a positive hole in the valence band. This process emits a photon at the wavelength of which is associated with the band gap:

$$\lambda = \frac{hc}{\Delta E_g}$$

where  $\lambda$  is the wavelength of the photon emitted,  $h$  is Planck's constant,  $c$  is the speed of light in a vacuum, and  $\Delta E_g$  is the band gap energy. Since the band gap energy of GaN is 3.4 eV, the wavelength of the photon that is emitted is 365 nm, which is in the violet/ultra violet part of the spectrum.

One of the experimental approaches used to obtain the specific wavelength of light emitted from a semiconductor material is to excite the electrons with an electron beam inside an scanning electron microscope (SEM). This process is known as cathodoluminescence (CL). Figure 2 shows the CL spectrum of a GaN nanowire. The band edge wavelength is observed at approximately 370 nm, but the dominant intensity of light is centered around 580 nm due to defects in the material. The purer the material, the less defect luminescence will be present [9]. It is this emitted luminescence under electron beam excitation that will be used to image charge transport.

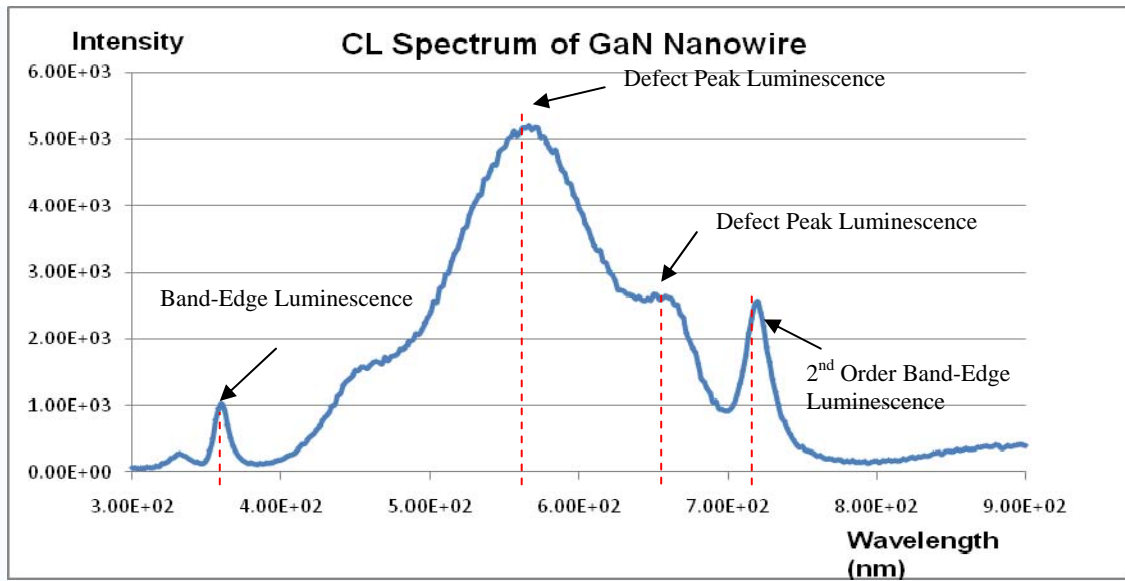


Figure 2. CL Spectrum of GaN Nanowire. From [9].



### **C. IMAGING CHARGE TRANSPORT**

While CL measures the intensity of the emitted light, it does not provide information on where the light is emanating from. Only with transport imaging can the spatial information from a fixed point of excitation on a structure be determined. Imaging the charge transport will provide added characterization information.

Traditional diffusion length measurements involved using electron beam induced current measurement (EBIC). The experimental set-up requires the semiconductor to be contacted and placed inside an SEM. The electron beam excites the semiconductor and creates electron-hole pairs. The charge would diffuse and whatever portion of the charge reached the contacts would be measured by an ammeter. However, this method is spatially restricted to the region adjacent to the contact. Also, contacting nanowires is a very time consuming task. With this technique, researchers have determined the diffusion lengths in GaN films range from 0.2  $\mu\text{m}$  in p-type films to be 1-2  $\mu\text{m}$  in n-type films [10].

Instead of measuring the diffusion length with EBIC, the diffusion length can be measured by capturing the CL spatially along the semiconductor with an optical sensor. This is the unique approach that the Naval Postgraduate School has developed and demonstrated successfully with solar cell materials.

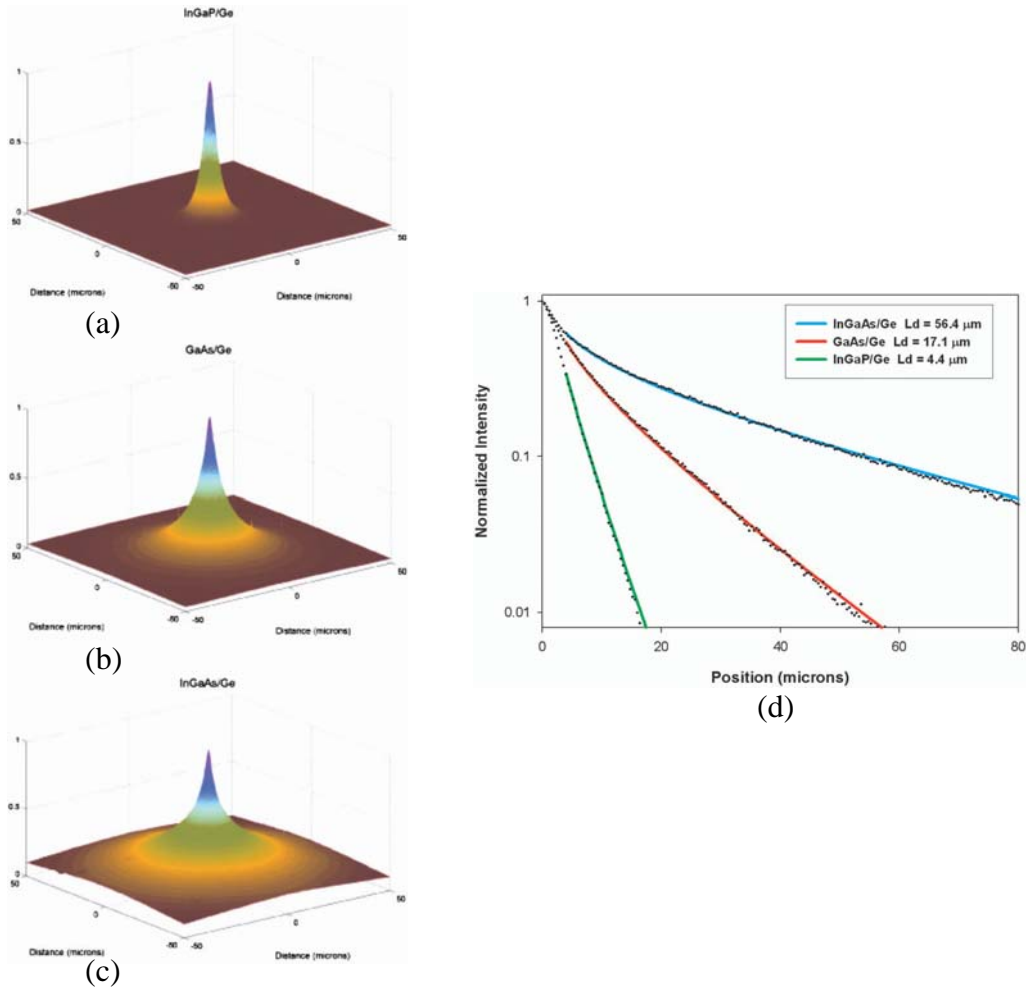


Figure 3. Minority carrier diffusion in (a) InGaP (b) GaAs (c) InGaAs with (d) semilog plot showing calculated diffusion lengths. From [11]

The material is placed inside the SEM and excited with the electron beam. Electron hole pairs are created and the minority carriers diffuse. When they recombine, CL is generated and captured with an optical CCD camera. The left side of Figure 3 shows the recombination distribution in InGaP, GaAs and InGaAs films with diffusion lengths of 4.4, 17.1, and 56.4  $\mu\text{m}$ , respectively. The semi-logarithmic plot on the right of Figure 3 shows the diffusion length analysis [11]. The CCD camera provides rapid results without contacting the sample. This technique can also be used to discover defect areas.

However, when attempting to study the diffusion length with CCD imaging on GaN nanowires, the pixel resolution is not high enough to make a proper measurement, since the CCD camera collection is in the far field. The diffraction limit limits the spatial resolution to approximately half the wavelength [12]. Figure 4 shows two GaN nanowires being scanned with an electron microscope and imaged with a Si CCD. Each pixel maps to a region of approximately 400 nm, which is close to the diffraction limit of the peak defect wavelength, and it is not small enough to conduct a spatially resolved measurement of the diffusion length which is expected to be approximately 1-2  $\mu\text{m}$  or less.

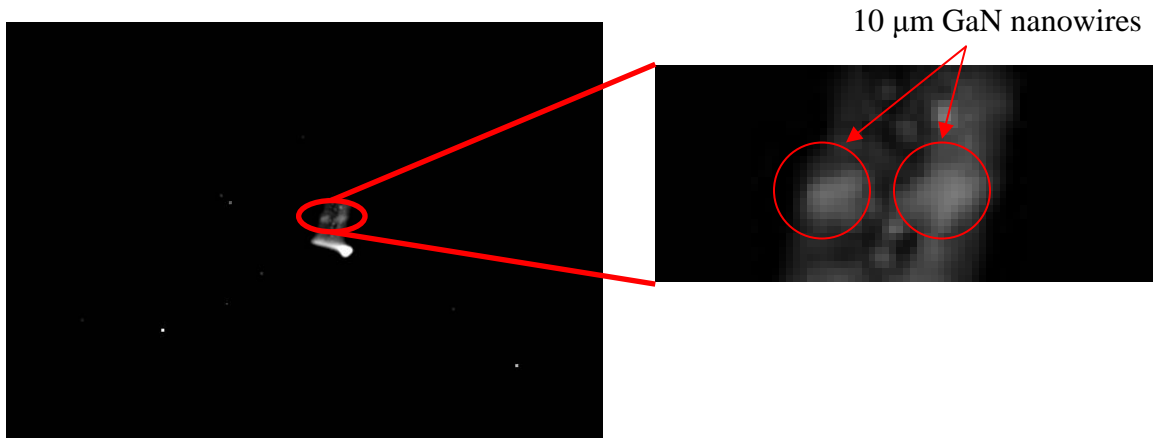


Figure 4. Optical picture of two 10 micron GaN nanowires with CCD camera.

#### **D. NEAR FIELD SCANNING OPTICAL MICROSCOPY (NSOM)**

Near Field Scanning Optical Microscopy (NSOM) is used to overcome the  $\lambda/2$  wavelength spatial resolution diffraction limit. Figure 5 shows the definition of far field and near field. To be able to measure a diffusion length of 1-2  $\mu\text{m}$ , a spatial resolution of approximately 50 nm would be required to do this accurately. This spatial resolution cannot be achieved in the far-field due to the diffraction limit.

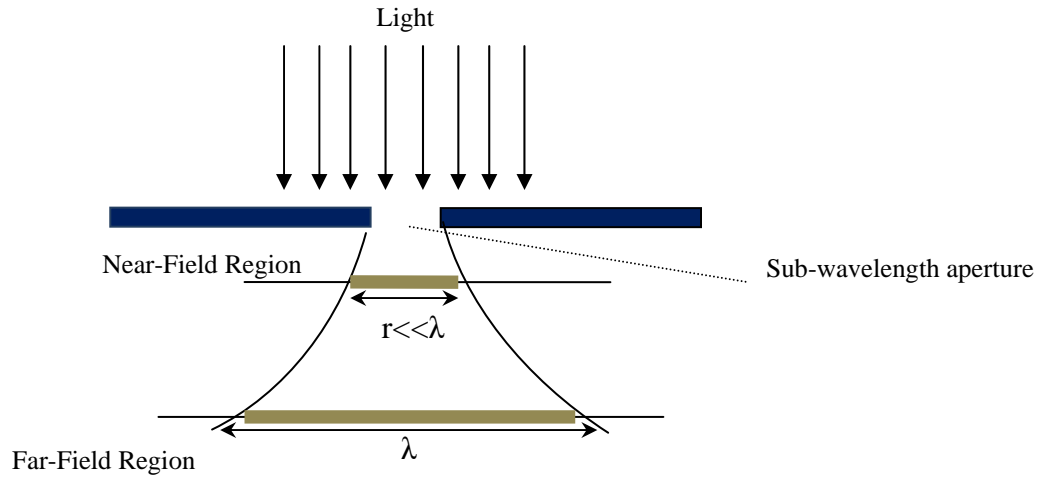


Figure 5. Definition of Far and Near field optics. From [9]

NSOM provides optical resolution much greater than the diffraction limit. An optical fiber is pulled to a 20–300 nm tip and metal coated, as shown in Figure 6, with a small hole in the metal coating at the end of the tip to provide a nano-scale aperture. This aperture is placed very close to the surface where the light is being emitted so the photons are not diffracted significantly before they enter the fiber optic. The photons are then transmitted to the detector to be counted. The distance from the surface must be much closer than the wavelength of the light. Light collection is strongly localized to the aperture and rapidly decays away from the opening [13]. The required region near the close contact with the surface is achieved by coupling the NSOM collection to an atomic force microscope.

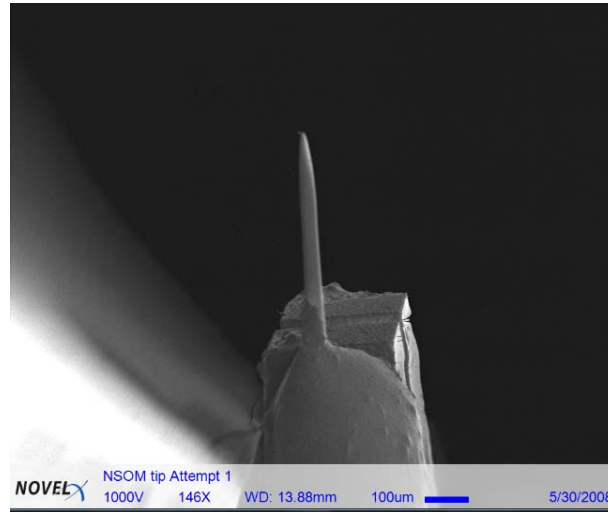


Figure 6. SEM picture of an NSOM tip.

#### **E. ATOMIC FORCE MICROSCOPY (AFM)**

Atomic Force Microscopy (AFM) is used for high resolution spatial mapping of the topography of nanostructures. This technique takes advantage of the short range chemical bonding forces and long range van der Waals forces. Figure 7 shows a plot of the short range forces and the long range forces as a function of the distance away from a structure. The AFM device in our system has a cantilever tip that is held fixed at some constant net repulsive or attractive force. When the tip encounters a change in height, the change in force is registered and recorded as a deflection [14] that provides feedback to maintain constant distance from the surface.

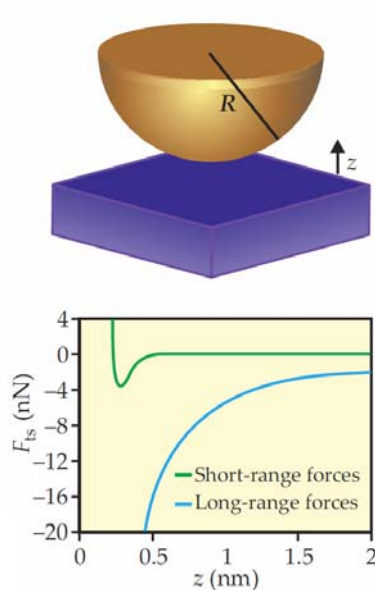


Figure 7. Forces acting on an AFM tip. From [14]

The Naval Postgraduate School uses an AFM from Nanonics LTD in which the cantilever is on a tuning fork. The cantilever is dynamically vibrating at the resonance frequency. This technique has less wear and tear on the tip, less noise in the signal, and provides greater deflection amplitudes. When used in the frequency modulation mode, any changes in the  $z$ -axis change the phase in the frequency, which is 10 times more sensitive than in amplitude mode. This combined AFM/NSOM system is described in detail in the next chapter.

THIS PAGE INTENTIONALLY LEFT BLANK

### III. EXPERIMENTAL SETUP

#### A. EQUIPMENT USED

This is one of the first attempts to create an integrated system with an AFM and an NSOM device inside a Electron Microscope [15] (see Appendix A). The original design criteria of these individual systems did not take into account operating in conjunction with each other. Therefore, initial operation is required to learn how the AFM and NSOM will interact with an electron beam. Understanding the performance of this new integrated instrument is just as important as the results themselves.

##### 1. Scanning Electron Microscope (SEM)

The scanning electron microscope (SEM) used for these experiments is a JEOL 840A. The electrons are thermionically emitted from a tungsten filament in an evacuated environment. These electrons are focused into a beam with a very fine focal spot and the diameter of the beam at the sample surface is a function of the probe current. Table 1 summarizes measured surface spot sizes at 30 keV in the SEM used for these experiments [16].

Probe Current (A)	16%-24% ( $2\sigma$ ) nm	FWHM (nm)
$3 \times 10^{-11}$	39	46
$1 \times 10^{-10}$	48	56
$3 \times 10^{-10}$	107	126
$1 \times 10^{-9}$	139	163

Table 1. 30 keV SEM beam with width diameter dependence on probe current. From [16]



Once the electron beam is focused, it passes through scanning coils in the objective lens, which deflect the beam horizontally and vertically. Understanding what happens after the electron beam is focused is critical to interpreting the results. There are three modes of operation used during these experiments:

***a. Picture Mode***

In picture mode, the scanning coils deflect the electron beam both horizontally and vertically in order to perform a scan in raster fashion over a rectangular area at a rate of 60 Hz. When the electron beam comes into contact with the sample, secondary electrons are emitted from the sample. The intensity variations of the secondary electrons associated with the topography are what provide the SEM picture [16]. Henceforth, the name of this mode is 'pic' mode. Any relative motion of the sample and the SEM beam can be immediately observed.

***b. Line Mode***

In line mode, the scanning coils deflect the electron beam in a horizontal direction only, in a raster fashion. There is no visual feedback mechanism in the line mode, therefore drift of the sample in this mode cannot be observed.

***c. Spot Mode***

In spot mode, the scanning coils deflect the electron beam down to a single point as directed by the operator. There is no imaging mechanism in the spot mode and any drift in the sample will not be observed.

**2. AFM/NSOM**

The Multiview 2000 built by Nanonics LTD is a flexible system that combines the AFM with the NSOM capabilities. It provides several features that are compatible with the unique requirements for conducting these transport imaging experiments inside an SEM environment:

***a. AFM Scanning Probe is an NSOM Fiber***

In order to collect the light and provide the AFM 3D topography data, the NSOM fiber also performs as the AFM probe. Figure 8 is a schematic diagram of the AFM/NSOM probe together. The tuning fork cantilever incorporates the NSOM tip which provides the desired near-field optical resolution and the spatial/topography resolution information needed for accurate diffusion length measurements.

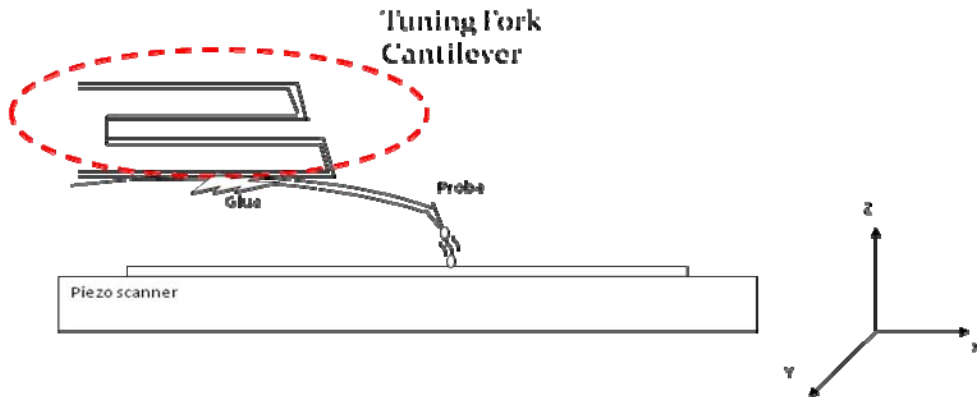


Figure 8. Schematic Diagram of the AFM/NSOM probe. From [9]

***b. Optical Access to the Sample***

The electron beam must be able to reach the nanowire in order to create the electron-hole pairs. The Multiview 2000 has an unobstructed optical axis allowing the SEM beam to excite the sample as shown in Figure 9. Most AFM systems do not provide this unobstructed view to the sample since they use a laser-mirror combination to monitor motion of the AFM probe. This configuration does not provide optical access for an SEM beam.

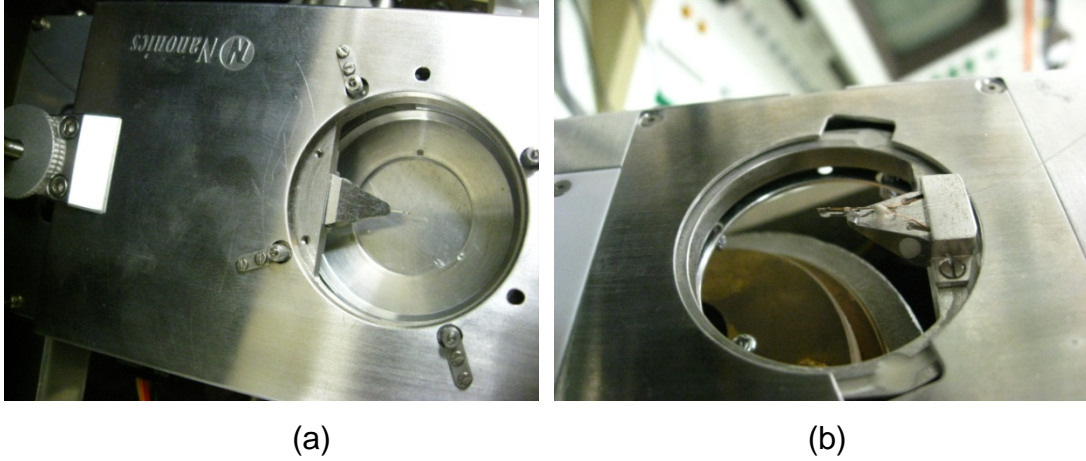


Figure 9. Top (a) and Reverse (b) Views of the AFM/NSOM Probe Attached onto the MultiView 2000 Scanner.

*c. Independent Scanning Plates*

The AFM portion has dual independent scanners for both top and bottom plates. Common AFM machines fix the top scanner, where the probe resides, and use the lower plate to scan the sample. Our experiments require a fixed incident electron beam relative on the sample to measure the diffusion lengths. Figure 10 shows the basic components of the MultiView 2000 in the JEOL 840A system.

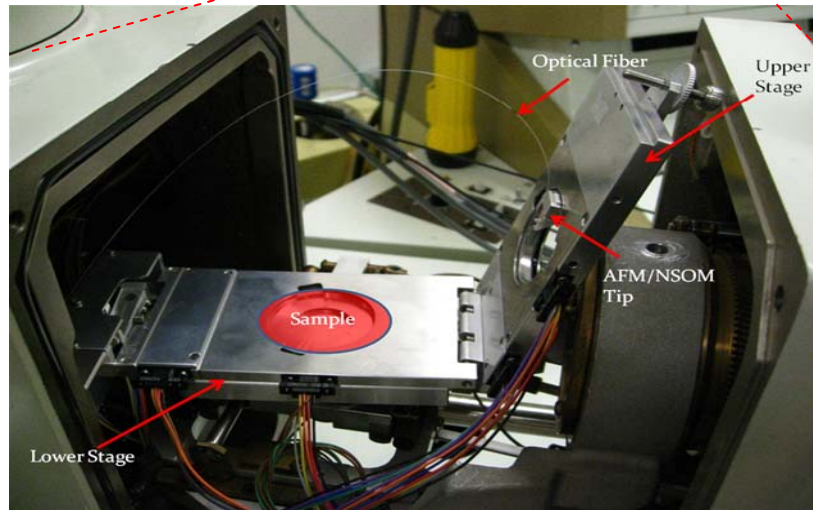
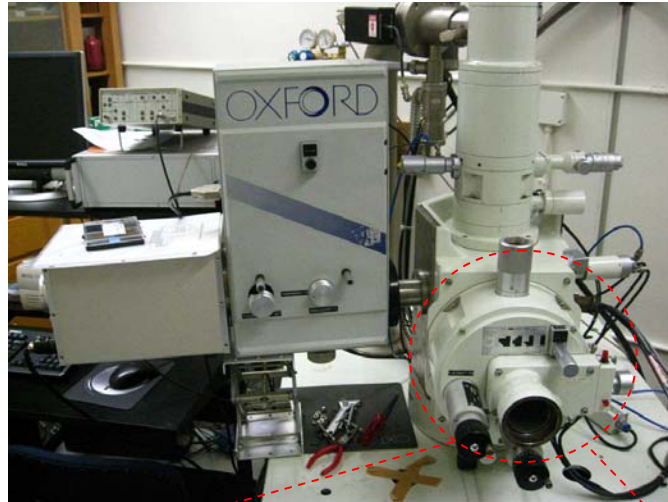


Figure 10. Nanonics MultiView 2000 Scanner in the JEOL 840 SEM.

The Nanonics 2000 features the top plate scanning capability which decouples the SEM beam excitation from the NSOM light collection. This allows the beam to be fixed on the sample while the NSOM tip scans it, collecting the optical signal.

***d. MultiView 2000 Specifications***

Sample Scanner	Piezoelectric Based Flat Scanner (3D Flat Scanner™) Height 7mm
SPM Scan Range	X and Y direction Up to 200 microns
	Z- direction Up to 70 microns
Scanner Resolution	< 0.005 nm in the z axis
	< 0.015 nm in the x and y axis
Motor Controller	High voltage peizo drivers (HVPD) with low voltage adaptor and Scanning probe microscopy controller that contains Proportional, Integration, and differential measurements. (see Figure 11)
Cantilever length	300-1000 $\mu\text{m}$
Resonance Frequency	80-390 kHz
Aperture size	200 - 300 nm
Transmission Wavelength	0.193 - >10.5 $\mu\text{m}$
Photon counter	Si single photon detector (see figure 11)

Table 2. MultiView 2000 specifications. From [17]

The photon counter is a Si single photon detector, Figure 11 (b), with a fiber optic termination which needs to be aligned carefully to provide enough luminescence for analysis. Its can detect light over the 400 to 1060 nm wavelength range.



(a)



(b)

Figure 11. (a) Counterclockwise from Top Left Corner: Low Voltage Adapter, HVPD for Upper Stage, SPM Controller, HVPD for Lower Stage and Counter and Power Supply for the APD. (b) The APD for Detecting Photons from the Fiber Probe During Measurements.

## B. EXPERIMENTAL APPROACH

The unique coordination of SEM and AFM/NSOM provides spatial imaging over a very wide range of scale—mm to sub nm. This cannot be achieved with either instrument alone. In addition, it provides the ability to control charge generation with a degree of spatial resolution that is difficult to achieve with optical systems.

The JEOL 840A SEM is used to find the nanowires. Once a wire is identified, the SEM beam is placed into spot mode, creating the electron hole pairs at the desired point of interest on the nanowire. The AFM/NSOM is used to collect the photons from recombination and map their intensity along the nanowire as illustrated in Figure 12.

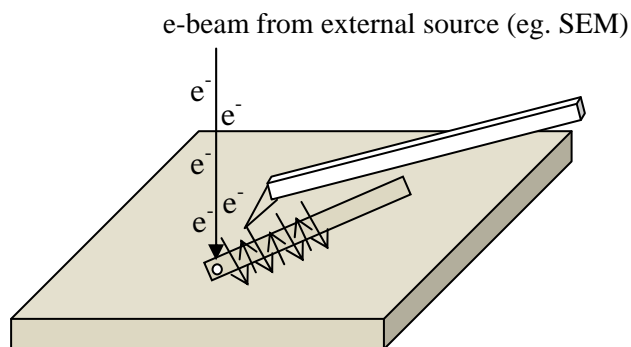


Figure 12. NSOM Scan with an Externally Excited Generation Source. From [9]

## 1. Considerations

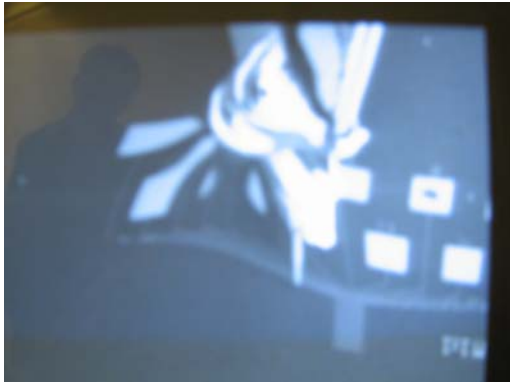
There are several pitfalls that need to be considered addressed to obtain accurate results, given the high degree of stability and resolution required in these experiments.

### *a. Grounding of the Sample*

As with anything that enters an SEM, it is critical to have the proper grounding of the sample. Given that the sample holder sits on three plastic pedestals to allow for inertial motion that enables sample positioning, the sample is electrically isolated from the rest of the system. Placing a grounding strap from the sample to the stage will mitigate major charging issues in the SEM. However, local charging near the tip can remain an issue.

### *b. Grounding of the NSOM Tip*

Ensuring that the NSOM tip is grounded is just as critical as ensuring the sample is grounded. The glues on the tip that holds the fiber to the cantilever are insulators and when the SEM beam hits these glue spots, a charge builds up which deflects the SEM beam if the associated field is large enough. Figure 13 demonstrates this phenomenon.



(a)



(b)

Figure 13. SEM pictures (a) demonstrating NSOM glue charging and distorting picture and (b) showing minimal distortion.

Eliminating the glue is not an option. Therefore this distortion is a part of the experiment that has to be dealt with. Each tip charges differently and the operator must adjust to maximize the data collection without too many artifacts. The effect that is seen while scanning is slight movement of the SEM image, indicating some relative motion of the incident beam. This movement has been documented to range from negligible to 1500 nm.

If the movement is negligible to 100nm, the SEM can be used in spot mode to create electron hole pairs and the NSOM tip can scan without fear of the SEM beam moving off the nanowire. Figure 14 shows the NSOM results from a SEM spot mode where the SEM excitation is located at the top of the nanowire.



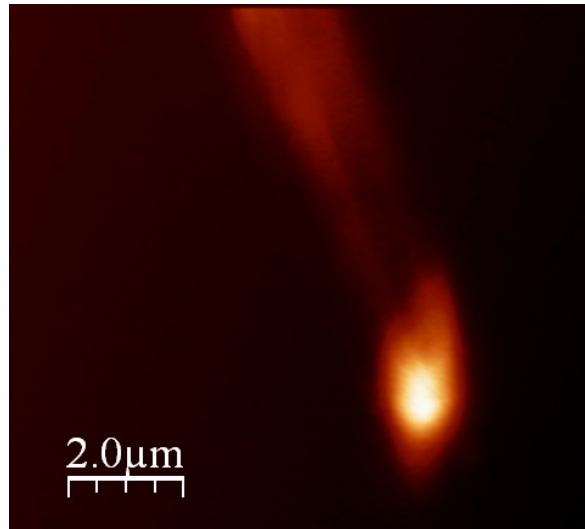


Figure 14. NSOM picture captured using 'spot' mode.

However, if there is sample/beam movement greater than 100 nm, there is a possibility that, while conducting a scan, the SEM beam in spot mode will walk off the sample, giving poor results. Therefore, line or pic mode must be used to ensure the SEM excitation point stays fixed. Which excitation mode to use is dependent on the direction of movement. If the movement is parallel to the movement of the scanning tip, line mode would be the mode of choice. If the movement is in any direction other than parallel with the scanning probe, 'pic' mode is recommended. In this mode, the SEM operator can see any drift movement and compensate for it.

Since the SEM beam is now being rastered in some fashion and is no longer hitting a single excitation point with a steady stream of electrons, this introduces a sinusoidal artifact in the NSOM picture as seen in Figure 15 (a).

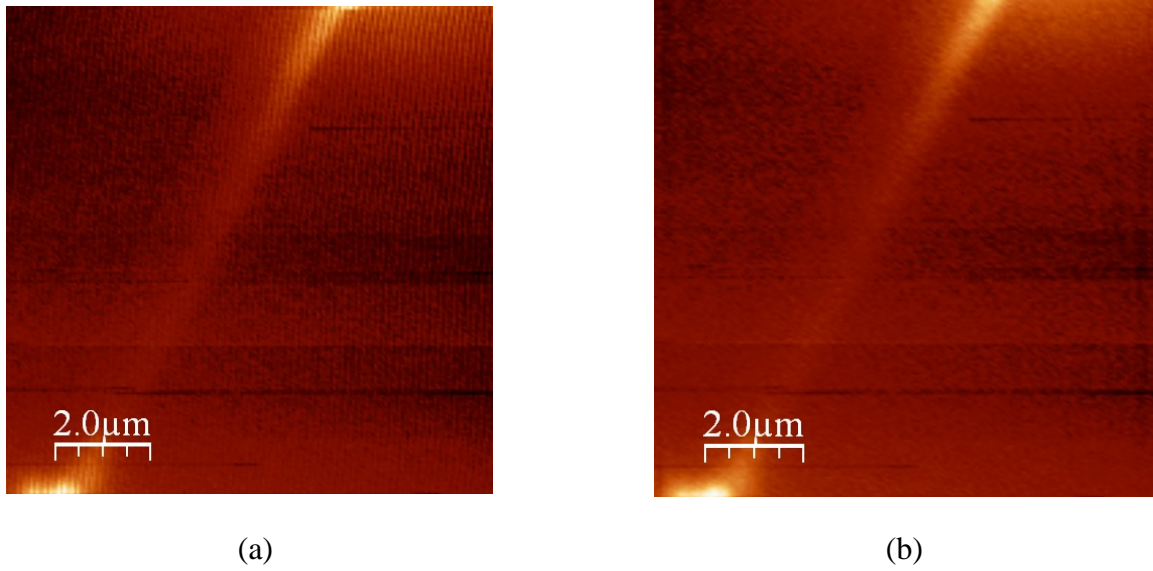


Figure 15. (a) Raw and (b) corrected NSOM data captured in 'pic' mode.

To correct for this sinusoidal artifact, the Fast Fourier Function in the WSxM 4.0 [19] software was used to remove the SEM beam raster frequencies in the image. Figure 15 (b) shows the results of this frequency cutting.

### *c. Interactions between the NSOM Tip and the Nanowire*

Both the NSOM tips and the nanowires are delicate structures. The NSOM is designed to scan close to structures, and use the strong and weak forces to maintain a certain distance from the surface. The nanowires are dispersed on a silicon wafer and are only held on to the substrate with van der Waals forces. If not optimized in feedback mode correctly, the NSOM tip will not adjust quickly enough and will move or break the nanowire. Figure 16 shows the dimensions of a typical nanowire and the NSOM tip.

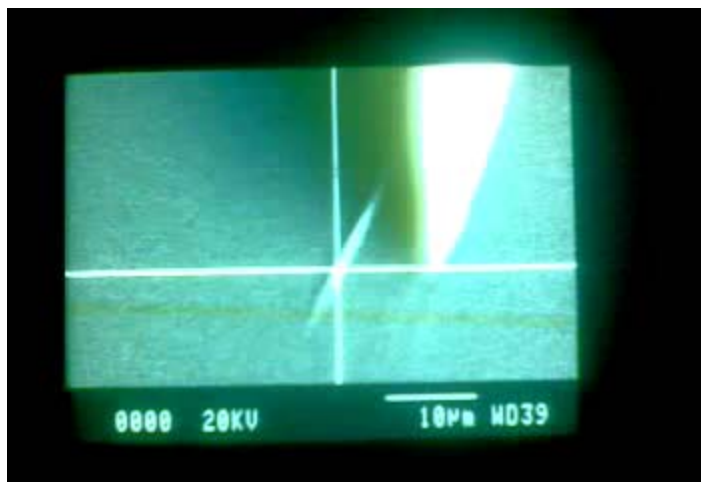


Figure 16. Dimension of a typical nanowire and the NSOM tip.

To avoid moving or breaking the nanowire, the lock-in procedures for the AFM portion of the MultiView 2000 need to be set up in the following conditions:

Feedback mode	Phase
Total gain	<10
Set point prior to approach	+0.25 to +0.35
Approach speed	300 Hz

Table 3. AFM settings to optimize contact between NSOM tip and nanowire

To properly conduct scanning operations, the operator must perform 'lock in' procedures. While in the lock-in portion of the program, operator must select the 'phase feedback' and then conduct a sweep in the 'magnitude sweep' centered around the given resonance frequency of the AFM/NSOM tip. One then adjusts the OSC gain to keep the highest amplitude between a magnitude of 8.0 and 8.5, while maintaining the total gain below 10. Once amplitude has been set, the "auto phase" function is initiated. After "auto phase" is complete, conduct a 'phase sweep' to and adjusting the frequency

cursor to a frequency that its phase shift is just slightly negative is the last step in the 'lock in' procedures. Once the set frequency button has been depressed, the lock-in mode can be exited.

Even with these settings, the NSOM tip can still crash into the nanowires. The set point can be adjusted while in contact. The more positive the set point, the more force is applied to the NSOM tip. Therefore, to avoid NSOM and nanowire damage, the set point needs to be negatively adjusted. However, if the NSOM tip receives too much negative setting, the AFM probe will lose contact with the sample and will lose contact with the sample and will not register any spatial data in the Z direction.

THIS PAGE INTENTIONALLY LEFT BLANK

## IV. MATERIALS

### A. GALLIUM NITRIDE

Gallium nitride (GaN), part of the III-V nitrides group, is a direct bandgap semiconductor. This direct bandgap semiconductor is the backbone of several optoelectronic devices such as light emitting diodes (LED) in the blue to ultra violet spectrum. The power-efficiency of these LEDs exceeds ordinary incandescent lamps in many large volume applications, such as traffic lights/signs and large displays. It is also being used for 'Blue Ray' DVD players due to its higher data transfer rate. GaN lasers are still under development, but show great promise in significantly better lifetimes than the blue-green based lasers [20].

The material properties of GaN also make it an ideal for electronic applications. These devices are good drift velocity ( $>2.9 \times 10^7$  cm/s at room temperature), have good electron mobility ( $\sim 2000$  cm<sup>2</sup>/V s at room temperature), good thermal conductivity (1.3 cm<sup>2</sup>/V s at room temperature) and can handle high frequencies ( $> 10$  GHz) [20].

#### 1. Growth Details

The GaN nanowires used in these experiments were grown using metal-organic chemical vapour deposition (MOCVD). Figure 17 below illustrates the growth process. The process begins with the melting of dispersed metallic crystals on sapphire inside a quartz tube furnace. The introduction of the product gasses controlled by mass controllers causes the saturation of molten metal droplets, which leads to the continuous precipitation of a single crystalline nanowire, as shown in Figure 18 [3].

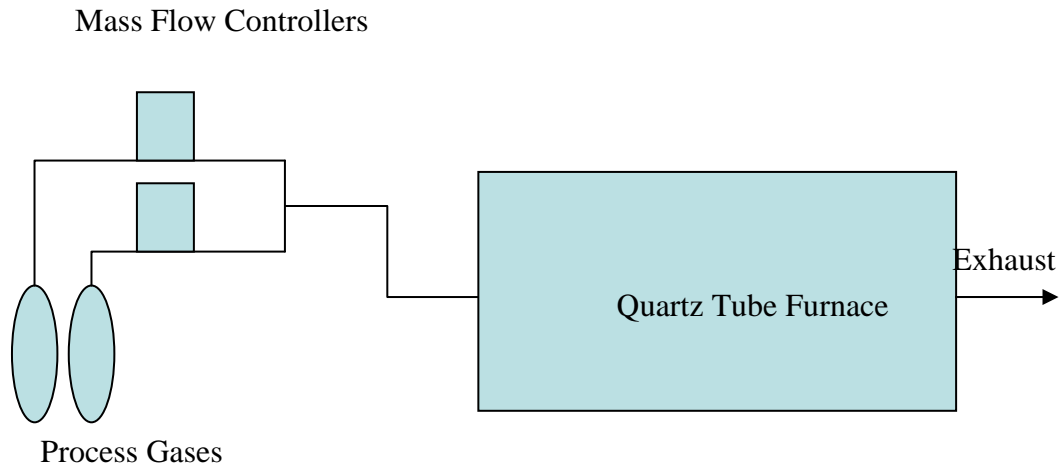


Figure 17. Illustration of MOCVD process. From [3]

The MOCVD growth technique provides doping control, reproducibility, facilitated scalability and can be integrated with film technology. Crystal growers at Sandia National Laboratory believe this to be the most promising method for controlled growth of III-nitride nanowires [21].

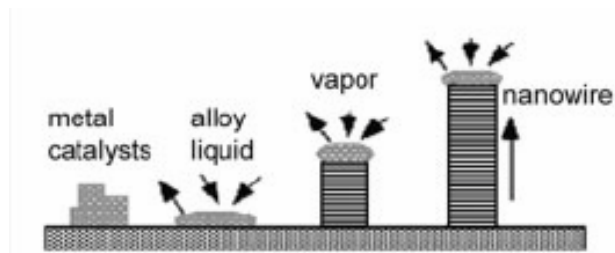


Figure 18. Growth process for a nanowire in the quartz tube furnace. From [22]

## 2. GaN Nanowire Characteristics

The GaN nanowires tested at the Naval Postgraduate School were grown by Ni-catalyzed MOCVD at 900°C on the r-plane. SEM images indicate typical length of GaN nanowire specimens ranged from 5 to 30  $\mu\text{m}$  in length, with diameters varying from  $\sim 100$

to 800 nm. Most wires are tapered, as shown in Figure 19 (a). Transmission electron microscopy indicates the nanowires are single crystalline, free of threading dislocations and have a triangular cross-sections (as shown in Figure 19 (b)) with a [1120] growth orientation.

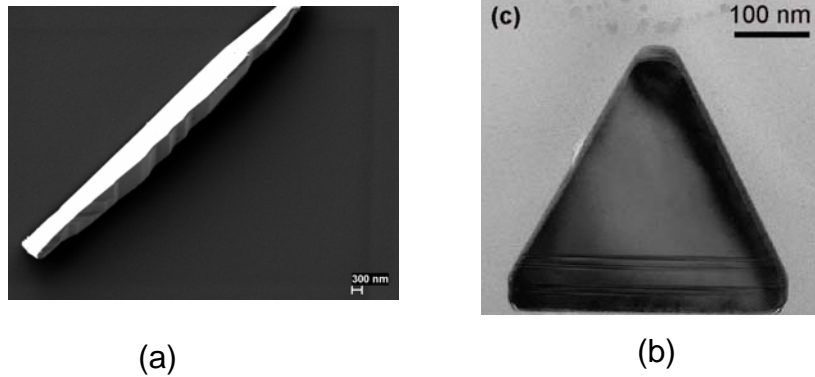


Figure 19. (a) and (b) are SEM picture of GaN nanowire showing the length and cross section characteristics. From [21]

For the GaN-AlGaIn core-shell nanowires, an AlGaIn layer approximately 15-20 nm thick, as determined by transmission electron microscopy, was subsequently grown around the GaN nanowire as a passivation layer at 1050°C for 480 s, with hydrogen as the carrier gas [21].

It is also critical to understand the dopant levels of the GaN nanowires prior to making measurements. N-type materials contain more electrons in the conduction band than the non-doped material. P-type materials have more positive holes in the valence band than non-doped materials. Both n-type and p-type semiconductors are needed to make electronic devices, such as transistors, op-amps and LEDs. In the case of an LED, a n-type and a p-type materials are placed together and the interface between the two materials creates a depletion zone. If the LED is forward biased, the electrons that are injected in the conduction band will recombine with a positive hole in the valence band, creating a photon [23].



GaN is easily grown as an N-type material. The unintentionally doped (UID) GaN nanowires are expected to be n-type due to possible oxygen contamination in the growth process and a relatively high formation enthalpy. These conditions add a shallow donor at 35 meV [20].

P-type GaN is more difficult to obtain. In the GaN nanowires used in these experiments, Mg acceptors were added during the growth process. However, dopant levels were not verified. These conditions add a shallow acceptor at 225 meV. In bulk materials, Mg doping has resulted in impurity banding effects which have been observed in CL spectra. Also, these impurities increase the disorder in the material. High concentrations of Mg cause mobility of the majority carriers to be low, at  $\sim 15 \text{ cm}^2 / \text{V s}$  [20].

For NSOM, the wires are dispersed onto a Si wafer. Si is a good substrate material because it has no significant luminescence signature of its own under electron beam excitation.

## **V. EXPERIMENTAL RESULTS**

### **A. GAN/ALGAN CORE-SHELL NANOWIRES**

To begin transport imaging with GaN nanowires in the near field, the Nanonics MultiView 2000 must be installed in the JEOL 840 SEM with a sample of GaN nanowires dispersed on a Si wafer. After the completion of the setup parameters discussed in Chapter III, a 30 $\mu$ m GaN/AlGaN core-shell nanowire with a 600 nm was found. Dimensional measurements were based on SEM imagery.

The SEM beam was focused near the end of the nanowire,  $\sim 6\ \mu$ m from the wire's edge. The SEM beam excitation condition was 20 kV with a probe current of  $3 \times 10^{-10}$  A and the SEM was operated in picture mode at  $\sim 35$ kX to keep the SEM beam on the same position on the wire.

Figure 20 (a) shows a 2-dimensional (2D) AFM image of topography of  $\sim 6\ \mu$ m of the 30  $\mu$ m long GaN/AlGaN nanowire. The height of the nanowire shows 720 nm, which is consistent with the SEM dimensional data; however, the width at  $\sim 1.5\ \mu$ m does not correlate with the SEM dimensional data. Width data from the AFM is not as reliable due to the relatively large tip used in NSOM compared to standard AFMs. The result is a convolution of the diameter of the wire and the diameter of the NSOM tip. The NSOM tip for this experiment was 250 nm.

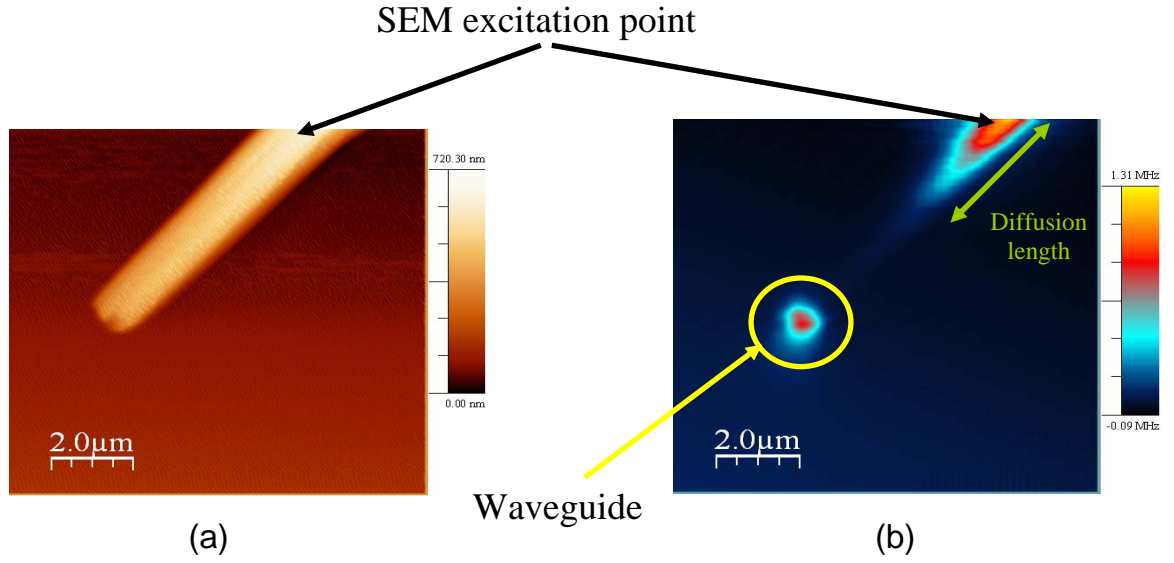


Figure 20. Topography (a), near-field luminescence and (b) image from a GaN nanowire under point source excitation. The image dimensions are 10 μm x 10 μm.

Figure 20 (b) depicts the NSOM intensity from the recombination of the diffused minority carriers as a function of position. The SEM electron beam was held fixed at a point near the top of the image and diffusion of light can be seen along the axis of the GaN nanowire. Figure 21 shows a combined AFM/NSOM 3-dimensional (3D) image combining the data from the 2D pictures in Figure 20. Results show that the carrier diffusion shown in the NSOM measurement follows the topographical features of the GaN nanowire.

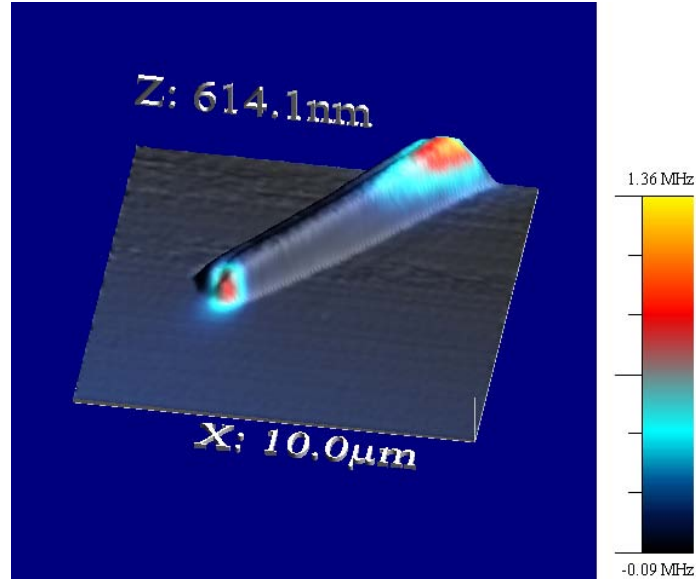


Figure 21. 3-D combination of topography and near-field luminescence from a GaN nanowire under point source excitation.

The near circular light intensity on both Figure 20 (b) and 21 at the end of the GaN nanowire shows the evidence of waveguiding. When electron-hole pairs recombine, a photon is created and the distribution of the emanating light is in  $4\pi$  as shown in Figure 22 (a). The portion of the light that is captured by NSOM tip for the purpose of diffusion length measurements are the photons leaving the nanowire close to vertical. The rest of the photons are trapped inside the nanowire due to total internal reflection (refractive index of GaN is greater than the vacuum inside the SEM). Figure 22 (b) shows an NSOM intensity measurement on a  $\sim 10 \mu\text{m}$  GaN nanowire with SEM beam excitation in the middle of the wire. There is clear evidence of waveguiding at both ends of the nanowire depicted by the purple circles. The large NSOM signal off to the right of the nanowire is an artifact of the NSOM tip being directly hit by the SEM beam during the scan. This direct hit of the SEM beam with the fiber optic creates light inside the fiber itself, providing a false reading of light from the sample. This region should be ignored.

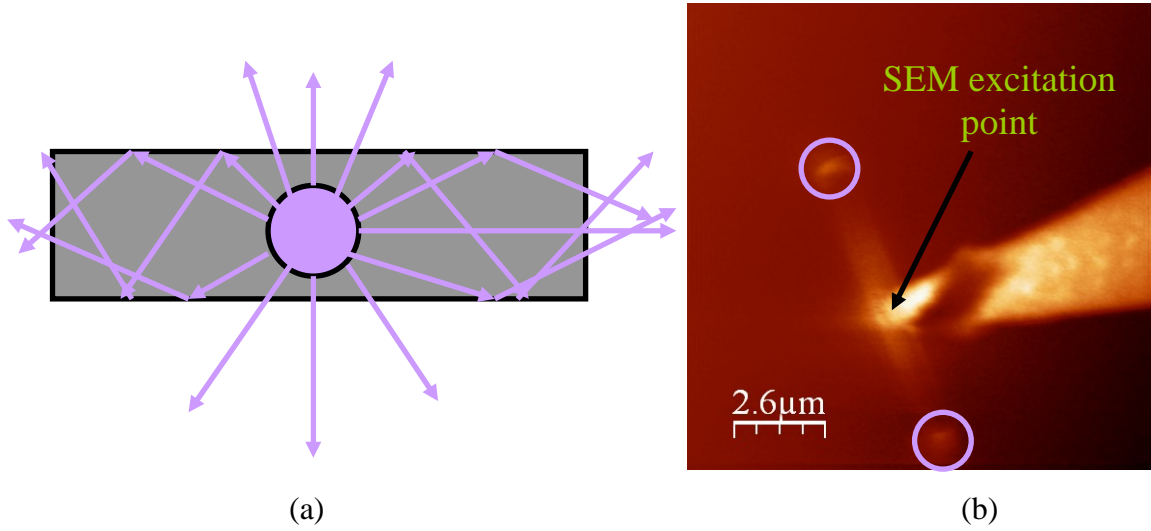


Figure 22. (a) Depicts how a nanowire will waveguide light and (b) show NSOM intensity data on a GaN nanowire with SEM excitation point in the middle and evidence of waveguiding at both ends.

Figure 23 shows the NSOM intensity as a function of distance from the SEM point of excitation on the GaN nanowire in Figures 20 and 21. Data are plotted on a linear (a) and semi-logarithmic (b) scale. The data showed an oscillation caused by relative movement in the electron beam and sample while scanning which can produce a sinusoidal artifact in the raw data. This was mitigated by analyzing the data in a logarithmic Fourier plot and removing the sinusoidal artifact. The diffusion length for this case was measured to be  $1.1 \pm 0.05 \mu\text{m}$  [24] (see Appendix B). This is consistent with the relatively large range of minority carrier diffusion lengths reported for n-type thin films of GaN,  $\sim 1\text{-}2 \mu\text{m}$  [10].

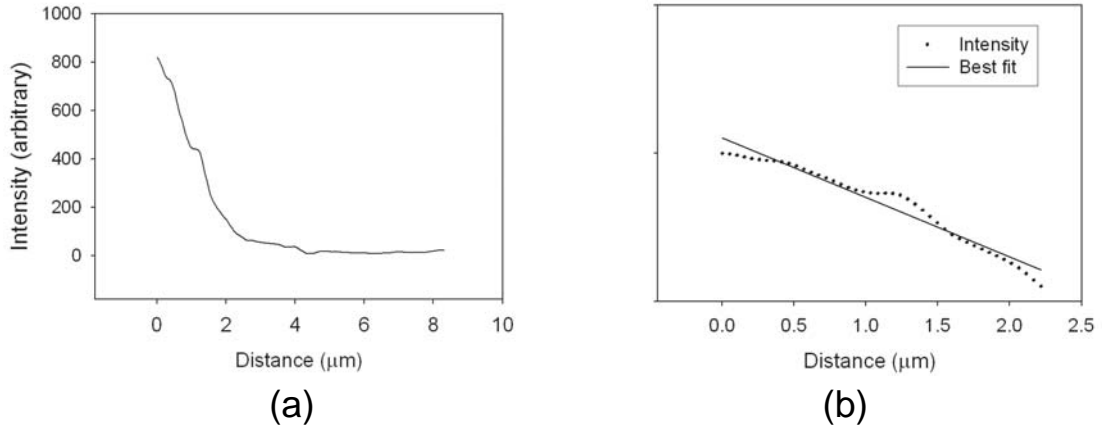


Figure 23. Intensity as a function of distance resulting from minority carrier in 1D resulting in minority carrier profiles. GaN wire diameter is 500 nm. Excitation conditions were 20 keV and  $3 \times 10^{-10}$  A probe current in line mode.

Figure 24 shows a series of measurements of the intensity distribution on a 10  $\mu\text{m}$  long wire, measured for excitation at a single spot as a function of probe current. Using the lower probe currents of  $6 \times 10^{-12}$  A and  $3 \times 10^{-11}$  A, extracted diffusion lengths of  $1.3 \pm 0.1$   $\mu\text{m}$  were consistent with results in Figure 24. However, as the probe current was increased to  $1 \times 10^{-10}$  A, the extracted diffusion length increased to 2.7  $\mu\text{m}$ . When the probe current was increased again to  $6 \times 10^{-10}$  A, the extracted diffusion length increased further to 3.1  $\mu\text{m}$ .

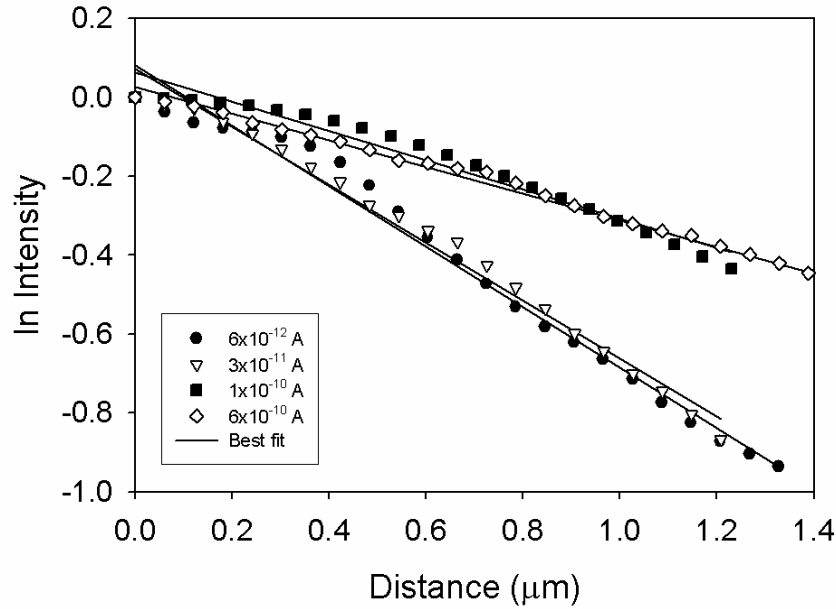


Figure 24. Intensities as a function of distance. GaN wire diameter is 700 nm. Excitation conditions were 20keV and different probe currents ( $6 \times 10^{-12}$ ,  $3 \times 10^{-11}$ ,  $1 \times 10^{-10}$ , and  $6 \times 10^{-10}$  A).

In transport imaging in epitaxial layers, an increase in excitation intensity can begin to affect the minority carrier diffusion length measurement if one moves out of the low injection regime and into a regime where the recombination lifetime becomes a function of the local excitation, due to the effect on the local majority carrier population. In this case, one normally observes a decrease in  $L_d$  at higher excitation. One assures operation in the low injection regime by measuring as a function of probe current until the measured value for  $L_d$  asymptotes to a constant value at the lower probe currents.

Results in Figure 24 illustrate a related, though different, challenge for the NSOM imaging measurements in proximity to an electron beam. The lower probe currents produce a consistent value for  $L_d$ . However once the probe current is raised above a certain value (which will change with each wire due to the dimensions and luminescent intensity), the diffusion length appears to increase as a function of the probe current. One explanation for this phenomenon is that higher probe currents result in higher intensity of scattered electrons from the incident beam. These electrons can interact with the NSOM

fiber causing direct excitation of luminescence in the silica material. This can also be addressed by moving to lower excitation currents. In the future, this effect can be further removed with the use of narrow band filters centered around the GaN band edge luminescence at 3.4 eV ( $\sim 360$  nm), since the broad emission from the fiber is located primarily in the 400-600 nm range. This assumes however that the band edge nanowire luminescence is sufficiently intense to compensate for the loss in broad band signal.

Another explanation for larger  $L_d$  with higher probe current could be that the SEM electron beam induces a surface charge on the GaN nanowire. This surface charge then repels the electrons in the conduction band, in essence, creating the image of a larger diffusion length. The higher the probe current, the more charge is deposited on the surface, creating a higher repulsion force on the electron.

## **B. UNCOATED GALLIUM NITRIDE NANOWIRES**

### **1. Unintentionally Doped (UID) GaN Nanowires**

Figure 25 shows the NSOM intensity as a function of distance from the SEM point of excitation on the UID GaN nanowire. Excitation conditions were 20 KeV and  $3 \times 10^{-10}$  A probe current in line mode. Data is plotted on a semi-logarithmic scale. The data showed an oscillation caused by relative movement in the electron beam and sample while scanning which produce a sinusoidal artifact in the raw data. This was mitigated by analyzing the data in a logarithmic Fourier plot and removing the sinusoidal artifact. Even after the removal of the oscillation data, the signal to noise ratio was low compared to the light output intensity of GaN/AlGaIn core-shell nanowires. The diffusion length for this case was measured to be  $1.1 \pm 0.2 \mu\text{m}$ .



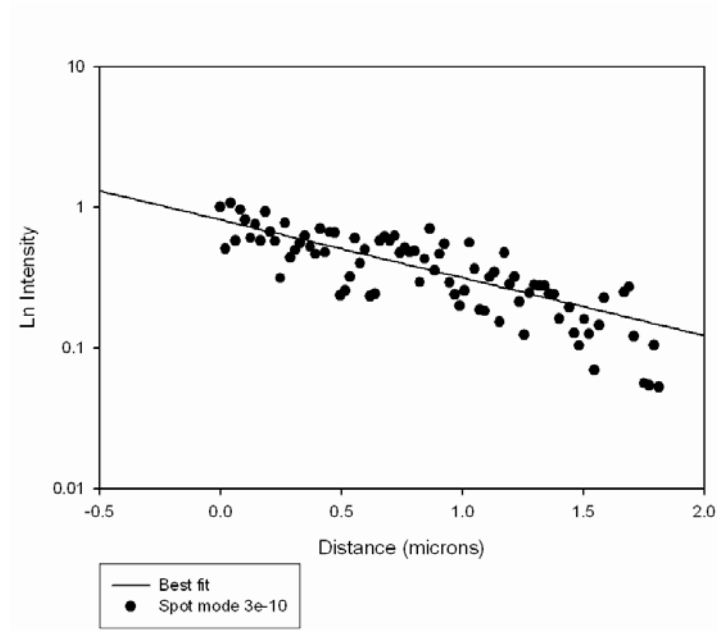


Figure 25. Intensity as a function of distance resulting from minority carrier in 1D resulting in minority carrier diffusion profile. UID GaN wire diameter is 600 nm. Excitation conditions were 20 keV and  $1 \times 10^{-10}$  A probe current in line mode.

Figure 26 shows the NSOM intensity as a function of distance from the SEM point of excitation for two other UID GaN nanowires. Excitation conditions were 20 KeV and  $1 \times 10^{-10}$  A probe current in line mode and  $3 \times 10^{-10}$  A probe current in spot mode. Both UID nanowires were 600 nm in width. The diffusion length for this case was measured to be  $0.81 \pm 0.2 \mu\text{m}$  and  $1.1 \pm 0.2 \mu\text{m}$  respectively. This directly supports the theory that the higher probe currents create the appearance of a larger diffusion length due to surface charge and/or the scattering of the SEM beam onto the fiber. However, the probe current could not be further lowered to confirm this hypothesis since the NSOM intensity at the lower probe currents did not rise above the noise.

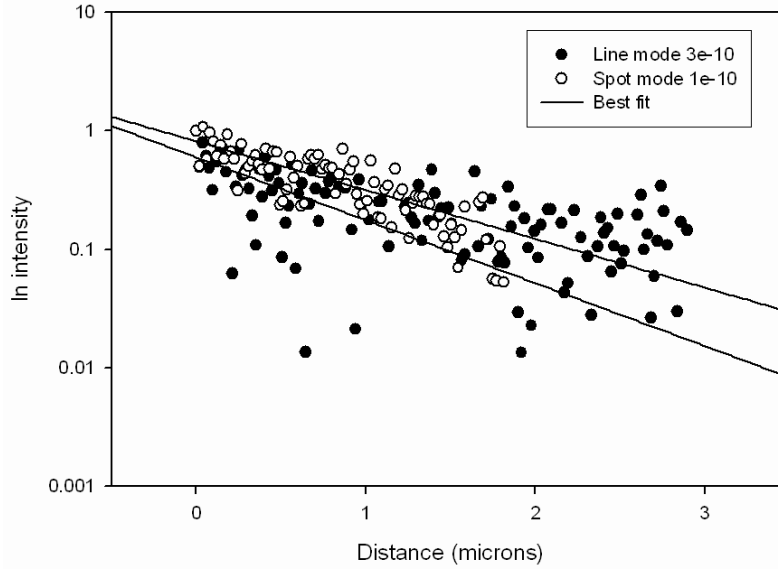


Figure 26. NSOM Intensity as a function of distance of two UID GaN wire with diameters 600 nm each. Excitation conditions were 20keV and different probe currents ( $3 \times 10^{-10}$ , and  $1 \times 10^{-10}$  A).

### C. MAGNESIUM DOPED (P-TYPE) GAN NANOWIRES

Figure 27 shows the NSOM intensity as a function of distance from the SEM point of excitation on the p-type GaN nanowire. Excitation conditions were 20 KeV and  $3 \times 10^{-10}$  A probe current in spot mode. Data are plotted on a semi-logarithmic scale. The signal to noise ratio of the light intensity is again low compared to GaN/AlGaN core-shell nanowires. The diffusion length for this case was measured to be  $0.71 \pm 0.2 \mu\text{m}$ .

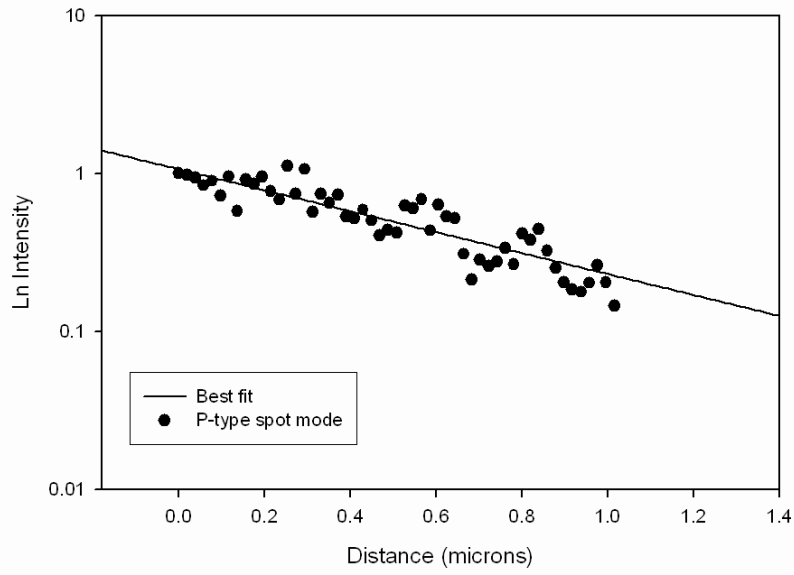


Figure 27. NSOM Intensity as a function of distance of a P-type GaN wire with diameter is 800 nm. Excitation conditions were 20 keV and  $6 \times 10^{-10}$  A probe current in line mode.

Figure 28 shows the NSOM intensity as a function of distance from the SEM point of excitation for the same p-type GaN nanowire however using the three different SEM modes: spot, picture, and line. Excitation conditions were 20 KeV and  $6 \times 10^{-10}$  A probe current. The width of the p-type GaN nanowires was 600 nm. The diffusion length for spot mode was  $0.71 \pm 0.2 \mu\text{m}$ , picture mode was  $0.66 \pm 0.2 \mu\text{m}$ , and line mode was  $0.44 \pm 0.2 \mu\text{m}$ .

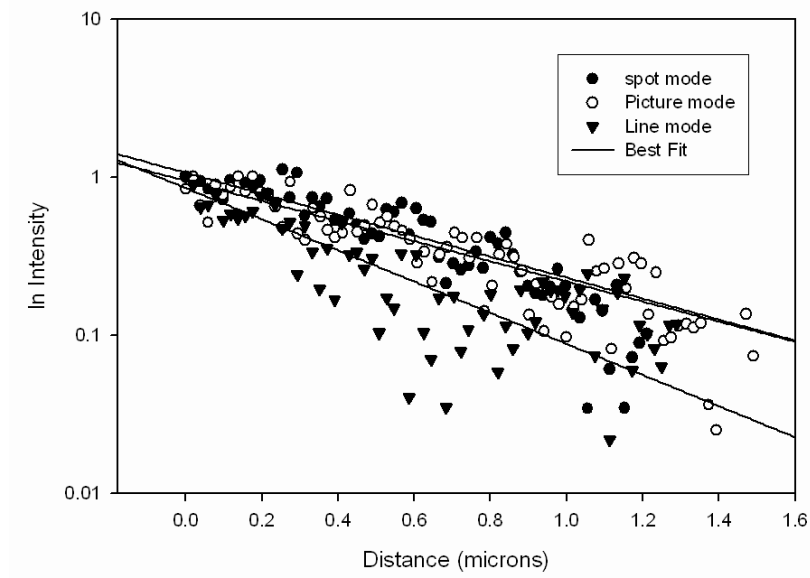


Figure 28. Intensities as a function of distance on three types of scans on the same p-type GaN wire. Wire diameter was 600 nm. Excitation conditions were 20 keV and  $6 \times 10^{-10}$  A probe current with different SEM modes (Spot, Picture, and Line).

THIS PAGE INTENTIONALLY LEFT BLANK

## VI. CONCLUSIONS AND SUGGESTIONS FOR FURTHER RESEARCH

### A. CONCLUSIONS

This thesis set out to determine the transport properties of the minority carriers in GaN nanowires by using AFM/NSOM with the Nanonics Multiview 2000 operating inside an SEM to image minority carrier diffusion. A summary of the results for measurement of minority carrier diffusion length is tabulated in Table 4.

<u>Diffusion lengths in GaN Nanowires</u>		
Nanowire	AFM/NSOM	EBIC
GaN/AlGaIn core-shell	1.3 +/- 0.20 $\mu\text{m}$	1.12 +/- 0.26 $\mu\text{m}$ [24]
UID GaN	0.96 +/- 0.25 $\mu\text{m}$	0.40 +/- 0.1 $\mu\text{m}$ [24]
P-Type	0.65 +/- 0.35 $\mu\text{m}$	Not tested

Table 4. Results for GaN diffusion lengths

The GaN/AlGaIn core-shell nanowires provided, by far, the most consistent results. The intensity of the electron-hole pair recombination was quite strong, well above the signal to noise ratio. In parallel, Maj. Chiou Perng Ong, of the Singaporean Army, conducted Electron Beam Induced Current (EBIC) measurements for his thesis research and provided very similar results which are also tabulated in Table 4. Consistent AFM/NSOM and the EBIC data give validity to these methods at determining the diffusion lengths.

The uncoated GaN nanowires, both UID and P-type, did not provide such optimal results. The intensities of the electron-hole pair recombination were weak since they did not bring the signal significantly past the noise level. Maj. Ong performed EBIC

measurements on the UID and came within 58% of the diffusion length measured from AFM/NSOM, which is denoted in Table 4. Additional measurements on more samples will be needed to obtain more reliable results on these materials.

## **B. SUGGESTIONS FOR FURTHER RESEARCH**

There is significant future research to be preformed on the characteristics of GaN nanowires and the use of AFM/NSOM inside an SEM environment.

### **1. Study of GaN Nanowire Waveguide Modes**

One of the more interesting discoveries was the near field imaging of waveguide phenomena in the GaN nanowires. Growers at Sandia National Labs have predicted this phenomena [25]. Figures 21(b), 22 and 23(b) directly confirmed that a GaN nanowire acts as an optical waveguide. Parallel experiments are needed to further analyze the waveguiding properties.

### **2. Transport Imaging of Charge with an Applied Electric Field**

It can be foreseen that these nanostructures will be placed in an electric field. Being placed under a bias changes the spatial location of recombination of the minority carriers. This combined effect of diffusion and drift behavior is a critical characteristic in understanding the behavior of this semiconductor structure. To conduct these experiments, a contacted nanowire with the contact spaced at least 5  $\mu\text{m}$  apart is needed in order for the AFM/NSOM tip to scan the nanowire without hitting the contacts.

### **3. Further Investigation on Diffusion Lengths in Other Materials**

The AFM/NSOM method is not restricted to GaN nanowires. This procedure can be used on any direct band gap materials to measure/image their transport behaviors. A good example of an alternative application is determining the depletion region on a P-N junction nanowire. In discussing the growth method of these types of nanowires with Sandia National Laboratory, it is not clear to them where the depletion region is located on the nanowire. The NSOM intensity would drop off dramatically at the depletion

region if one side of the P-N nanowire was stimulated by the SEM beam. This NSOM intensity variation could provide the growers an exact location of the depletion region.

#### **4. Optimization of Probe Tips to Limit Charge and Drifting Effects**

As discussed in Chapter III, the AFM/NSOM tip can greatly affect the results of NSOM data by deflecting the SEM beam. Experimenting on different types of AFM/NSOM tips, SEM and scanner configuration could provide crucial performance data which would enable the operator to optimize performance from the Nanonics MultiView 2000 in the SEM.



THIS PAGE INTENTIONALLY LEFT BLANK

# APPENDIX A. ARTICLE ON TRANSPORT IMAGING [15]

## Transport Imaging with Near-Field Scanning Optical Microscopy

Nancy M. Haegel\*, Chun-Hong Low, Lee Baird and Gwon-Hwee Ang  
Physics Department, Naval Postgraduate School, Monterey, CA 93943

### ABSTRACT

Direct imaging of charge transport is obtained in luminescent materials by combining the excitation capability and resolution of a scanning electron microscope (SEM) with high sensitivity optical imaging. A regular optical microscope (OM) or a near field scanning optical microscope (NSOM) is operated within the SEM to allow for characterization of semiconductor materials by imaging the spatial variation of luminescence associated with minority carrier recombination. The NSOM system uses a Nanonics MultiView 2000 that allows for independent scanning of both sample and collecting fiber. The technique builds upon traditional cathodoluminescence (CL), but differs in that spatial information from the luminescence is maintained, allowing for direct imaging of carrier transport. The approach will be introduced with results from double heterostructures of GaAs and the effect of radiation damage on minority carrier diffusion lengths. Then, its application to structures requiring near field imaging will be illustrated with results from measurements of carrier diffusion in GaN nanowires.

**Keywords:** Transport imaging, minority carrier, diffusion length, near field scanning optical microscopy, NSOM, nanowires

### 1. INTRODUCTION

The ability to image phenomena at an appropriate scale of resolution often provides important insight into our understanding of physical systems. This has been true when the phenomena of interest are relatively distant (e.g., telescopes), small (e.g., SEM or TEM) or otherwise invisible to the human eye (e.g. thermal imaging). The ability to directly observe what can otherwise only be assumed or inferred can challenge existing assumptions and lead to the discovery of new phenomena. In materials for optoelectronic applications, such as detectors, emitters, or solar cell materials, local transport phenomena such as carrier diffusion and drift play important roles in device performance. Historically, these transport parameters were measured in ways that provided spatially averaged values over macroscopic size samples. With the emergence of spatially resolved techniques such as cathodoluminescence (CL) and electron beam induced current (EBIC), it became clear that significant spatial non-uniformities associated with crystal growth or processing were often present. Characterization approaches need to keep pace with these spatial variations as well as the continuously decreasing device dimensions.

We describe here an instrument to "image transport" - to make phenomena such as minority carrier diffusion and drift, charge injection and localized field variations directly visible via optical imaging of the luminescence associated with charge recombination. The approach combines multiple microscopes - 1) a scanning electron microscope (SEM) to provide both high resolution sample imaging and charge generation, 2) an optical microscope and camera to image luminescence in the far field and 3) a near field scanning optical microscope (NSOM), with an optical fiber tip for light collection in the near-field.

#### 1.1 Related techniques

Although transport imaging is related to cathodoluminescence, there are fundamental differences between transport imaging and all of the scanning luminescence techniques. In both CL and transport imaging, the electron beam is used to generate electron-hole pairs in a semiconductor material. In standard CL, however, the incident beam is rastered and all light collected due to generation at a given point is mapped back to and assumed to be associated with that generation

\*nmhaegel@nps.edu; phone 1 831 656-3954; fax 1 831 656-2834

Scanning Microscopy 2009, edited by Michael T. Postek, Dale E. Newbury, S. Frank Platek, David C. Joy,  
Proc. of SPIE Vol. 7378, 73782B · © 2009 SPIE · CCC code: 0277-786X/09/\$18 · doi: 10.1117/12.824114

Proc. of SPIE Vol. 7378 73782B-1

Downloaded from SPIE Digital Library on 13 Nov 2009 to 205.155.65.226. Terms of Use: <http://spiedigitallibrary.org/terms>

point. While a large fraction of the photon signal from the recombination probably does, in fact, occur at or very near the point of charge generation, the actual spatial variation, resulting from any diffusion or drift of the charge, is lost in conventional CL. Transport imaging maintains that information by acquiring a spatially resolved image of the recombination, showing the extent to which the generated carriers have moved between the point of generation and the point of recombination.

The most famous example of indirect monitoring of transport in semiconductor materials is the classic Haynes-Shockley experiment, for the measurement of minority carrier drift length [1]. A pulse of excess minority carriers is created (optically or through an injecting contact) and the evolution of the pulse over time is monitored by measuring current flow at a location removed from the injection point. Values for minority carrier mobility and lifetime are obtained from the motion and spreading of the charge packet. Material uniformity between the contacts generally must be assumed. Transport imaging enables a direct two-dimensional visualization of the Haynes-Shockley experiment and is better suited to the size and nature of many of the epitaxial and nanoscale structures of today. Transport imaging in the SEM can provide spatially resolved measurement of transport parameters, a high degree of flexibility for both low to high bandgap materials and minimal sample preparation.

## 1.2 Related Experiments

Most experiments designed to take advantage of optical recombination to track motion of charge have used laser excitation. Höpfel et.al. imaged recombination in GaAs quantum wells to demonstrate negative mobility due to carrier drag in a high mobility hole plasma [2]. Bieler et. al. used spatially resolved photoluminescence to study sweep-out behavior in transient electric fields [3] and Logue et. al. used microPL to measure diffusion lengths in ZnCdSe/ZnSe quantum wells [4]. Boone et.al. applied local fields to attenuate luminescence within a defined aperture to demonstrate decreasing the duration of spontaneous emission in LEDs for high speed communications applications [5]. These examples demonstrate the broad applicability of transport imaging. Using the SEM provides this capability for a wide range of materials, since the electron beam can create electron-hole pairs in all types of luminescent materials and also takes natural advantage of the ease of control of the beam for charge generation. Transport imaging in the SEM would be capable of a wide range of high throughput programmable spatial mapping behavior.

## 2. DESCRIPTION OF THE EQUIPMENT

The optical systems are operated in conjunction with a JEOL 840 SEM. Figure 1 illustrates the approach schematically, with the far field system, using the optical microscope, shown at right and the near field system, using the NSOM, shown at left. In the OM system, the OM is placed directly under the pole piece in the SEM, using a retractable arm. The electron beam passes through the first optical collecting surface and is incident, as usual, on the sample surface. The optical microscope is a JEOL accessory that was initially designed for the independent fine adjustment of sample height required for wavelength dispersive X-ray spectroscopy (WDS). These OMs were designed with short focal lengths and normally used with a lamp source and video imager.

In transport imaging, the OM is used solely in a passive mode, detecting light emitted directly from the sample. The detector is a thermoelectrically cooled CCD camera. Cameras can be easily interchanged (e.g., to an InGaAs array to extend wavelength response), but the majority of the work has been done using a  $2184 \times 1472$  pixel Si CCD array, with a pixel size of  $6.8 \times 6.8 \mu\text{m}^2$ . The OM insert is a basic two lens system, modified to allow for passage of the electron beam. Resolution is close to diffraction limited, estimated to be  $\sim 0.56$  to  $0.22 \mu\text{m}$  for wavelengths ranging from 870 nm (GaAs band edge luminescence) to 350 nm (GaN band edge luminescence). The magnification is  $\sim 20\times$ , so the resulting effective scale for the optical images is  $\sim 0.4 \mu\text{m}/\text{pixel}$ . Defining the maximum pixel size  $\Delta x$  for optimum sampling as  $\Delta x \sim MR/2$ , where M is the magnification and R is the resolution, we find that  $\Delta x = 5.6 \mu\text{m}$  at  $\lambda = 870 \text{ nm}$  and  $\Delta x = 2.8 \mu\text{m}$  at  $\lambda = 350 \text{ nm}$ . Therefore the current system is resolution limited at infrared wavelengths and pixel size limited for the blue/UV.

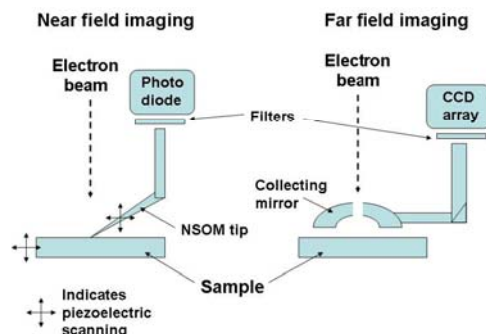


Fig. 1. Schematic diagram illustrating key components of the transport imaging for far field system (right) incorporating the optical microscope and near field (left) incorporating the NSOM. In both cases the collecting optics are within the SEM chamber, while the camera or photodiode is external to the chamber.

In principle, it would be possible to place a spectrometer in the optical path to differentiate recombination mechanisms during transport, such as various defect-related versus band-to-band emission. However, the loss of throughput suggests that appropriate combinations of bandpass filters are a better choice for wavelength selection in most cases. These filters can be used to eliminate, for example, substrate luminescence, or to select the emission of interest in a multilayer sample. Finally, in the OM system, the sample is mounted on a liquid helium cooled stage, with variable temperature capability from 5 to 300 K.

To move beyond the resolution limit imposed by diffraction, it is necessary to collect the luminescence in the near-field limit. To achieve this, the optical microscope is replaced by a near-field scanning optical microscope system. We utilize an instrument from Nanonics Imaging Ltd., the MultiView 2000, that provides capability for independent scanning of both sample and tip. To perform transport imaging in the near field, the electron beam is incident in a fixed location, as with the optical microscopy work described above, but now the light is collected through a fiber probe, operating simultaneously as the tip for atomic force microscopy (topography) and near-field optical collection. Therefore, the unique architecture of the MultiView 2000 is critical to the ability to scan the collecting probe, while keeping an independent generation source fixed at a point of interest on the sample.

The NSOM tips are Au coated cantilevered fiber tips with aperture diameters ranging from 100 to 300 nm. They are operated with tuning fork feedback with resonant frequencies in the 100 kHz range. Piezodrivers on both the sample stage and the probe stage allow for independent scanning of either sample or collecting tip over a range of up to  $\sim 70$   $\mu\text{m}$ . Resolution is determined primarily by tip aperture. The strong dependence of transmission on aperture size requires a trade-off between using the smallest possible apertures and collecting a sufficient amount of light, especially in transport experiments where light is collected at some distance from the point of carrier generation. In most work, we utilize tips with 200-300 nm diameter.

Prior to data collection, one can observe the scan area of the tip on the sample using the SEM imaging mode. During data acquisition for transport imaging, the SEM is again operated in spot mode and the NSOM tip scans the collection area of interest. A primary challenge in this work is to insure that the generation spot remains fixed - e.g. on the nanowire of interest - and that charging effects and other phenomena that would lead to sample drift are minimized. For some cases, the SEM is operated at high magnification, but still in scanning mode, so that the sample area can be imaged directly during the NSOM scan. Light is collected by the fiber and transmitted to a Si photodiode. Again, the option exists to insert various filters to select the luminescence of interest.

### 3. DIRECT IMAGING OF MINORITY CARRIER DIFFUSION

One primary application of transport imaging is to enable contact free measurements of minority carrier diffusion length. This is a key parameter for many devices, including solar cells, bipolar transistors and light emitting devices. For epitaxial thin films, as well as one-dimensional structures such as nanowires, transport imaging can determine this important materials parameter from a single luminescence image. The simplest analysis occurs when the measurement is performed in the low injection regime, i.e., when the population of generated majority carriers is significantly less than the equilibrium majority carrier population. If the diffusion length is comparable to or greater than the radius for charge generation, then diffusion of minority carriers will broaden the luminescence associated with minority carrier recombination. We illustrate this with examples using the OM system, for solar cell materials with relatively long minority carrier diffusion lengths.

Figure 2 shows a 3-dimensional image of the recombination luminescence from a double heterostructure sample of GaAs. The GaAs layer has a thickness of 1.9  $\mu\text{m}$ , with GaInP barriers on either side. The sample is p type with  $N_A = 9.7 \times 10^{15} \text{ cm}^{-3}$ . The structure is grown on a Ge substrate, reflecting the application of this type of material in high efficiency triple junction solar cells (GaInP/GaAs/Ge), produced primarily for space applications [6]. Charge was generated at the center point with a 20 kV beam and a probe current of  $6 \times 10^{-11} \text{ A}$ .

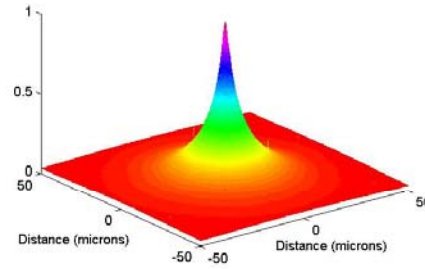


Fig. 2. Luminescence intensity ( $z$ ) as a function of position, resulting from recombination of charge in a double heterostructure of GaInP/GaAs/GaInP. The charge generation point is in the center of the distribution.

The minority carrier diffusion length can be extracted from the intensity distribution along any diameter. For diffusion from a steady state point source in two dimensions, the minority carrier distribution and resulting intensity profile will be given by

$$I = \frac{g}{2\pi L^2} K_0(r/L)$$

where  $K_0$  is the zeroth order modified Bessel function of the second kind,  $L$  is the minority carrier diffusion length,  $g$  is the excitation rate and  $r$  is the radial coordinate. We perform a least squares fit of the data to extract the value for  $L$ . For this material, the minority carrier diffusion length is determined to be 17.1  $\mu\text{m}$ . With an independently measured minority carrier lifetime of 20 ns from time resolved photoluminescence, the minority carrier mobility is found to be 5560  $\text{cm}^2/\text{Vs}$ . This type of imaging has been used to observe and quantify anisotropic diffusion in ordered alloys of GaInP, associated with variations in effective mass parallel and perpendicular to the ordering direction [7]. Minority carrier mobilities as a function of applied field in heavily doped p type GaAs heterostructures have also been determined using images of drift behavior [8].

### 3.1 Mapping effects of localized damage

The high degree of spatial control associated with charge generation in the SEM provides an ability to probe spatial variations in transport phenomena, as might be associated with localized defects or damage. In this way, phenomena such as radiation damage, which is often characterized extensively with structural techniques such as TEM or studied at the macroscopic scale via device failure, can be associated directly with local effects on electronic properties. To illustrate this capability, a several mm<sup>2</sup> region of a double heterostructure sample of p type GaInP/GaAs/GaInP (1.7 μm thick, with p type doping of  $1.7 \times 10^{16} \text{ cm}^{-3}$ , similar to the material from Figure 2 ) was exposed to a beam of 2 MeV protons to a dose of  $3 \times 10^{13} \text{ cm}^{-2}$  at 300 K.

Transport imaging was performed in regions directly within (A), on the border (B) and far removed (C) from the damaged region. The resulting 2 dimensional luminescence images are shown in Figure 3 (upper). The lower graph shows the intensity profile through the diameter for location B, showing the clear asymmetry in the diffusion behavior. Extracted minority diffusion lengths can be mapped from a maximum of 17.1 μm in the as-grown material to 3.1 μm in the center of the damaged region. This represents an ~ 80% decrease in minority carrier diffusion length, while the peak intensity of the luminescence at the corresponding locations decreased by only ~ 50%.

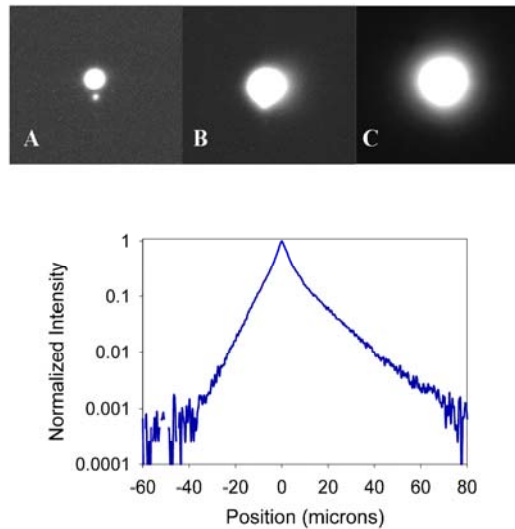


Figure 3. Luminescence images (upper) resulting from electron diffusion in A) radiation damaged, B) on the border of the radiation damaged region and C) as-grown GaAs. In all cases, image dimensions are 216 μm x 200 μm. In the lower figure, the intensity profile from location B is shown on a semi-logarithmic scale, illustrating the asymmetry in diffusion length resulting from the localized damage. The incident electron beam was 20 kV at  $6 \times 10^{11} \text{ A}$ .

## 4. TRANSPORT IMAGING OF NANOWIRES

Minority carrier properties are also critical in many of the applications being proposed for nanowires, such as light emitting diodes and lasers. Probing electrical properties of individual devices is challenging, requiring contacts to a single nanowire structure. While I-V characteristics have been measured for a range of devices and majority carrier mobility measurements are extracted from characterization of FETs, measurements of minority carrier properties are

very limited. Transport imaging with the NSOM provides one of few ways to acquire this information in a direct manner with no additional fitting parameters.

Figure 4 shows an SEM image of one of the GaN nanowires of interest. The image was taken with a NovaX MySEM with an imaging voltage of 1 kV. The wires range from 5–30  $\mu\text{m}$  in length, with diameters varying from  $\sim 100$ –500 nm. Wire diameter can vary along the length of a particular wire, as shown in the example below. The wires are GaN-AlGaIn core-shell nanowires, grown via Ni-catalyzed MOCVD [9].

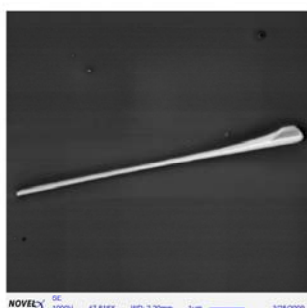


Fig. 4. SEM image (1 kV) of a GaN/AlGaIn core-shell nanowire. Magnification is 47,516X.

For transport imaging, the electron beam is fixed at a point on the wire and the NSOM is scanned over a region of interest. Topography and optical intensity of emitted light are collected simultaneously. Figure 7 shows a 3 dimensional image of the NSOM output from point excitation of a single GaN nanowire. The intensity of the collected light is plotted as a function of position in x and y over a 20  $\mu\text{m}$  x 20  $\mu\text{m}$  region. The electron beam was held fixed at a point at the upper part of the wire. Beam excitation conditions were 20 kV with a probe current of  $1 \times 10^{-9}$  A. The diameter of the wire at the point of excitation was approximately 200 nm, based on SEM and AFM imaging. One sees in the image both the luminescence associated with the diffusion of minority carriers along the wire, as well as the result of waveguiding of a portion of the luminescence along the wire, causing light emission at the end of the structure - approximately 10  $\mu\text{m}$  from the point of excitation. We assume that the luminescence is emitted in all directions. We collect a fraction that is emitted in the vertical direction. Because of the relatively broad and strong defect-related CL emission, a majority of the light is below band gap and is not expected to cause reabsorption and the generation of new carriers (photon recycling). This is supported by independent CL spectral studies under similar excitation conditions.

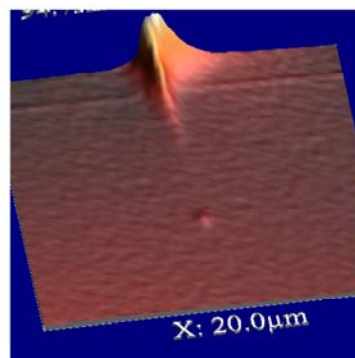


Fig. 5. Near-field luminescence image from a GaN nanowire under point source excitation. Image processed using WSxM [10] The image dimensions are 20  $\mu\text{m}$  x 20  $\mu\text{m}$ .

For diffusion in one dimension, the minority carrier distribution and resulting luminescence distribution is given by

$$I = (g/2L) \exp(-x/L)$$

where  $g$  is the generation rate and  $L$  is the diffusion length. The finite nature of the source can be incorporated by simply integrating over a Gaussian distribution for the generation region:

$$I = \frac{g}{2L} \sqrt{\frac{n}{\pi}} \int_{-\infty}^{+\infty} e^{-n\xi^2 + \frac{|x-\xi|}{L}} d\xi$$

where  $g$  and  $L$  are as previously defined,  $n$  determines the spread of the Gaussian source term and  $\xi$  is the integration variable. Majority carrier mobilities in n type, unintentionally doped GaN nanowires have been reported ranging from 2 to 600 cm<sup>2</sup>/Vs, depending on growth method [11] and diameter [12]. Minority carrier lifetimes also vary with diameter and growth conditions, but can be estimated to be on the order of 10<sup>-9</sup> s for wires of this diameter [13]. There are less data on hole mobilities, as most nanowires are n-type. Minority carrier mobilities in bulk materials are generally lower, but comparable order of magnitude to majority carrier mobilities. Order of magnitude, therefore, one expects diffusion lengths in the range from 100 to 1000 nm.

Figure 6 shows modeling results for diffusion from a ~ 200 nm generation region for one dimensional versus two dimensional geometries. Two cases are considered:  $L_{\text{diff}} = 300$  nm and  $L_{\text{diff}} = 1000$  nm. The same data are plotted on a semi-logarithmic scale in the right hand side of the figure. Diffusion lengths in the one-dimensional case can be extracted directly from the slope of the distribution. Although the one dimensional nature of the diffusion increases the absolute intensity at a given distance from the generation source, one sees that the intensity decreases rapidly for the shorter diffusion lengths, requiring the high density of data acquisition over a 1-2  $\mu\text{m}$  region that can only be obtained with the NSOM scanning.

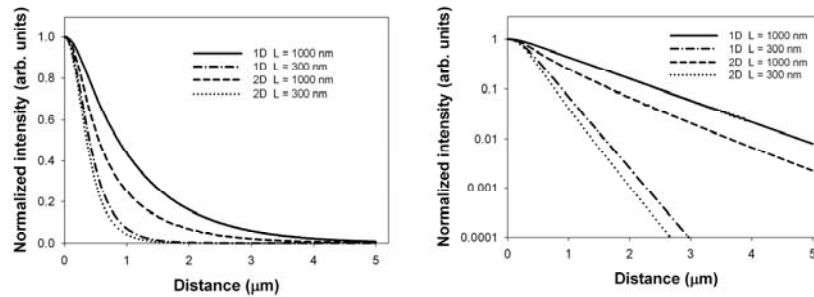


Fig. 6. Modeled diffusion profiles for diffusion in 1D and 2D from a Gaussian generation region, with standard deviation of 200 nm. Resulting minority carrier profiles are shown on linear (left) and logarithmic (right) axes.

Figure 7 shows the NSOM intensity from the image in Figure 5 plotted as a function of position along the wire. The exponential decay region closest to the point of excitation is extracted and plotted on a logarithmic scale in the right hand side of the figure. A linear regression was performed to extract the value of the slope. This produces a value of 0.63  $\mu\text{m}^{-1}$ , leading to a diffusion length of 1.6  $\mu\text{m}$ . This measurement reflects the quality of the material, the diameter of the wire at this position as well as the fact that these wires have an AlGaIn shell, which limits surface recombination effects. Future work will map the measured diffusion length along the full length of the wire, as well as study effects of shell layer material and thickness versus a free surface.



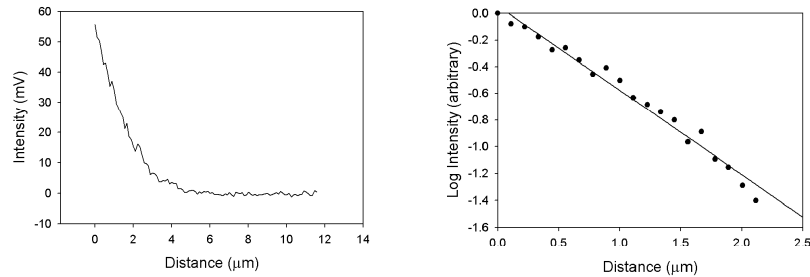


Fig. 7. NSOM intensity as a function of distance along the nanowire under point source excitation. At left, the intensity profile along a 12  $\mu\text{m}$  region. At right, a logarithmic plot of the intensity in the region adjacent to the excitation point.

In summary, we demonstrate a technique to provide direct imaging of minority carrier transport in a wide range of optically active materials. This has been used to measure minority carrier diffusion lengths in solar cell materials and demonstrate effects of local radiation damage. Transport imaging has also been demonstrated for the first time in GaN nanowires, using a combination of scanning near field microscopy and SEM. This technique provides both the optical sensitivity and the spatial resolution required to resolve diffusion lengths in novel materials and dimensionally confined structures.

## 5. ACKNOWLEDGEMENTS

This work was supported by NSF grants DMR-0526330 and DMR-0804527. We acknowledge many collaborators who have contributed to this work: R. King, H. Yoon and C. Fetzer of Spectrolab Inc. for solar cell materials, T. J. Mills, formerly at NPS, for transport measurements, K.M. Yu of Lawrence Berkeley National Laboratory for performing the proton irradiation, A. A. Talin and George Wang of Sandia National Laboratories for providing the GaN nanowires, and C. Scandrett and C. Frenzen of the Department of Applied Mathematics at NPS for contributions to the data analysis.

## REFERENCES

- [1] Haynes J. R. and Shockley W., "The mobility and life of electrons and holes in germanium," *Phys. Rev.* **81**, 835 (1951).
- [2] Höpfel R. A., Shah J., Wolff P. A., and Gossard A. C., "Negative absolute mobility of minority electrons in GaAs quantum wells" *Phys. Rev. Lett.* **56**, 2736 (1986).
- [3] Bieler J., Hubner J., Oestreich M., Kock M., Hin G., Pierz K. and Siegner, U., "Quantifying the drift velocity of carrier ensembles in time-dependent electric fields," *J. Appl. Phys.* **91**, 9869 (2002).
- [4] Logue F P, Fewer D T, Hewlett S J, Heffernan J F, Jordan C, Rees P, Donegan J F, McCabe E M, Hegarty J, Taniguchi S, Hino T, Nakano K, and Ishibashi A., "Optical measurement of the ambipolar diffusion length in a ZnCdSe-ZnSe single quantum well," *J. Appl. Phys.* **81**, 536 (1997).
- [5] Boone T. D., Tsukamoto H. and Woodall J. M., "Intensity and spatial modulation of spontaneous emission in GaAs by field aperture selecting transport," *Appl. Phys. Lett.* **82**, 19 (2003).
- [6] King R.R., Law D.C., Edmondson K.M., Fetzer C.M., Kinsey G.S., Yoon H., Sherif R.A., Karam N. H., " 40% efficient metamorphic GaInP/GaInAs/Ge multijunction solar cells," *Appl. Phys. Lett.* **90**, 183516 (2007).

- [7] Haegel N. M., Mills T. J., Talmadge M., Scandrett C., Frenzen C. L., Yoon H., Fetzer C. M., and King R. R., "Direct imaging of anisotropic minority-carrier diffusion in ordered GaInP," *J. Appl. Phys.* **105**, 023711 (2009).
- [8] Lubner, D. R., Bradley F.M., Haegel N. M., Talmadge M., Coleman M. P., and Boone T. D., "Imaging transport for the determination of minority carrier diffusion length," *Appl. Phys. Lett.* **88**, 163509 (2006).
- [9] Wang G. T., Talin A. A., Werder D. J., J. R., Creighton, Lai E., Anderson R. J., and Arslan I., " Highly aligned, template-free growth and characterization of vertical GaN nanowires on sapphire by metal-organic chemical vapour deposition," *Nanotechnology* **17**, 5773 (2006).
- [10] Horcas, I. Fernandez, J.M. Gomez-Rodriguez, J. Colchero, J. Gomez-Herrero, and A.M. Baro, "WSXM: A software for scanning probe microscopy and a tool for nanotechnology," *Review of Scientific Instruments* **78**, 013705 (2007).
- [11] Motayed A., Davydov A. V., Mohammad S. N., and MeIngailis J., "Experimental investigation of electron transport properties of gallium nitride nanowires," *J. Appl. Phys.* **104**, 024302 (2008).
- [12] Motayed A., Vaudin M. Davydov A. V., MeIngailis J., He M. and Mohammad S. N., "Diameter dependent transport properties of gallium nitride nanowire field effect transistors," *Appl. Phys. Lett.* **90**, 043104 (2007).
- [13] Chin A. H., Ahn T. S., Li H., Vaddiraju S., Bardeen C., Ning C. Z., and Mahendra K., "Photoluminescence of GaN nanowires of different crystallographic orientations," *Nanoletters* **7**, 626 (2007).

THIS PAGE INTENTIONALLY LEFT BLANK

# APPENDIX B. ARTICLE ON GALLIUM NITRIDE NANOWIRE DIFFUSION LENGTH WITH NSOM [24]

Author's personal copy

Physica B 404 (2009) 4933–4936



Contents lists available at ScienceDirect

Physica B

journal homepage: [www.elsevier.com/locate/physb](http://www.elsevier.com/locate/physb)



## Imaging minority carrier diffusion in GaN nanowires using near field optical microscopy

Lee Baird<sup>a</sup>, G.H. Ang<sup>a</sup>, C.H. Low<sup>a</sup>, N.M. Haegel<sup>a,\*</sup>, A.A. Talin<sup>b</sup>, Qiming Li<sup>c</sup>, G.T. Wang<sup>c</sup>

<sup>a</sup> Physics Department, Naval Postgraduate School, Monterey, CA, USA

<sup>b</sup> Sandia National Laboratories, Livermore, CA, USA

<sup>c</sup> Sandia National Laboratories, Albuquerque, NM, USA

### ARTICLE INFO

#### Keywords:

Transport imaging  
Minority carrier  
GaN nanowires  
Diffusion length  
Near-field scanning optical microscopy  
NSOM

### ABSTRACT

A novel system has been developed for the imaging of carrier transport within semiconductor nanostructures by operating a near field scanning optical microscopy (NSOM) within a scanning electron microscope. Luminescence associated with carrier recombination is collected with high spatial resolution to monitor the motion and recombination of charge generated by use of an electron beam as an independent point source. Light is collected in the near field from a scanning fiber using tuning fork feedback in an open architecture combined AFM/NSOM system allowing independent motion of sample and tip. From a single image, it is possible to obtain a direct measure of minority carrier diffusion length. This technique has been used in the near-field collection mode to image the diffusion of holes in n-type GaN–AlGaIn core-shell nanowires, grown via Ni-catalyzed MOCVD. Measurements were made on tapered nanowires ranging in diameter from 500 to 800 nm, with lengths up to  $\sim 30 \mu\text{m}$ . The average 1-dimensional carrier diffusion length was measured to be  $1.2 \pm 0.2 \mu\text{m}$  in the low injection limit. In addition, it is possible to map the luminescence that is waveguided to the end of the structure, imaging waveguide modes.

Published by Elsevier B.V.

### 1. Introduction

GaN and its alloys are used extensively in optoelectronics and nanowires based on GaN and the III-nitrides material system have recently been synthesized and investigated as potential nanoscale elements in optoelectronics and high-power, high-temperature, and high-speed devices [1,2]. However, as devices shrink in dimension towards the nanoscale, both optical and electronic materials properties change. One critical electronic transport parameter, minority carrier diffusion length, can be directly measured at the nanoscale by imaging charge transport.

The minority carrier diffusion length is instrumental to the performance of devices such as bipolar transistors, solar cells, and lasers. It can also be a measure of the quality of the material. One approach to determine minority carrier diffusion length is electron-beam-induced current (EBIC). However, the material needs to be electrically contacted and the experimental results provide a spatial average that is restricted to regions adjacent to the contacts.

The scanning electron microscopy (SEM)-based technique of imaging charge transport presented here measures the minority

carrier diffusion length by imaging the spatial variation of the recombination luminescence arising from carrier generation at a quasi point source. This paper presents, for the first time, measurements of the carrier diffusion length in GaN nanowires with an outer AlGaIn shell layer using this technique. The nanowire is excited locally with a steady-state SEM beam and luminescence is collected by an optical fiber scanned in the near field along the GaN/AlGaIn core-shell nanowire. This approach is basically an optical Haynes–Shockley experiment [3], but with a resolution determined by the near-field optical collection.

### 2. Description of the equipment

The optical imaging systems are operated in conjunction with a JEOL 840 SEM. Fig. 1 illustrates the approach schematically, with a far-field system, using the optical microscope (OM), shown at right and the near-field system of interest in this work, using the near-field scanning optical microscope (NSOM), shown at left. In the OM system, the OM is placed directly under the pole piece in the SEM using a retractable arm. The electron beam passes through the first optical collecting surface and is incident on the sample surface. The resulting luminescence is imaged by a Si CCD camera. This type of imaging has been applied recently to image

\* Corresponding author.  
E-mail address: [nmhaegel@nps.edu](mailto:nmhaegel@nps.edu) (N.M. Haegel).

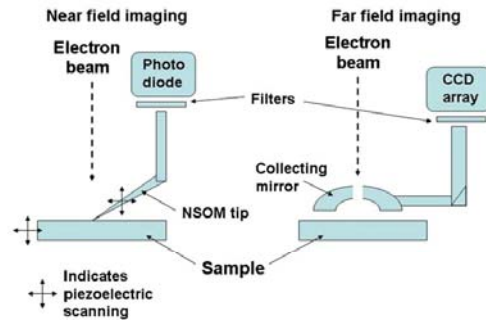


Fig. 1. Schematic diagram illustrating key components of the transport imaging for far field system (right) incorporating the optical microscope and near field (left) incorporating the NSOM. In both cases the collecting optics are within the SEM chamber, while the camera or photodiode is external to the chamber.

anisotropy of diffusion in ordered GaInP [4] and the drift of holes in heavily doped GaAs heterostructures [5]. One limitation for the far-field system is resolution. Based on the magnification of the microscope and the pixel size on the CCD, the maximum resolution is  $\sim 400$  nm/pixel.

To move beyond the resolution limit imposed by diffraction, it is necessary to collect the luminescence in the near-field. We utilize an instrument from Nanonics Imaging Ltd., the MultiView 2000, that provides capability for independent scanning of both sample and tip. The electron beam is incident in a fixed location and the light is collected through a fiber probe, operating simultaneously as the tip for atomic force microscopy (topography) and near-field optical collection. The unique open architecture of the MultiView 2000 is critical to the ability to scan the collecting probe, while keeping an independent generation source fixed at a point of interest on the sample. High voltage piezo drivers are used to control the upper and lower stages as well as the probe in three dimensions. The MultiView 2000 is capable of scanning an area of  $70 \mu\text{m} \times 70 \mu\text{m}$  and it uses proportional, integration, and differential (PID) controls. The PID controls are critical to set scanning conditions to avoid breaking or bending the GaN nanowires.

The NSOM tips are Au-coated cantilevered fiber tips with aperture diameters ranging from 100 to 300 nm, and are operated with tuning fork feedback with resonant frequencies in the 100 kHz range. The strong dependence of transmission on aperture size [6] requires a trade-off between using the smallest possible apertures and collecting a sufficient amount of light, especially in transport experiments where light is collected at some distance from the point of carrier generation. For the AFM/NSOM of nanowires, tips with 200–300 nm diameter work best.

Prior to data collection, one can observe the scan area of the tip on the sample using the SEM imaging mode. During data acquisition for transport imaging, the SEM is operated in spot mode and the NSOM tip scans the collection area of interest. A primary challenge in this work is to insure that the generation spot remains fixed—e.g. on the nanowire of interest—and that charging effects and other phenomena that would lead to sample drift are minimized. For some cases, the SEM is operated at high magnification, but still in scanning mode, so that the sample area can be observed during the NSOM scan. Light is collected by the fiber and transmitted to a Si photodiode.

### 3. Transport imaging of GaN nanowires

Fig. 2 shows an SEM image of a typical GaN/AlGaIn nanowire of interest. The image was taken with a NovaSEM. Imaging voltage was 1 kV. Typical GaN/AlGaIn nanowires in our specimen range from 5 to  $30 \mu\text{m}$  in length, with diameters varying from  $\sim 100$  to  $800$  nm. Many wires are tapered, as shown in Fig. 2. The n-type GaN–AlGaIn core-shell nanowires were synthesized by first growing the GaN nanowire core at  $900^\circ\text{C}$  by Ni-catalyzed metal-organic chemical vapor deposition (MOCVD) on *r*-plane as described in detail previously [7–9]. An AlGaIn layer approximately 15–20 nm thick, as determined by transmission electron microscopy, was subsequently grown around the GaN nanowire as a passivation layer at  $1050^\circ\text{C}$  for 480 s, with hydrogen as the carrier gas. Transmission electron microscopy indicates the nanowires are single crystalline, free of threading dislocations, and have triangular cross-sections with a  $[11\bar{2}0]$  growth orientation.

For transport imaging, the electron beam is fixed at a point on the wire and the NSOM is scanned over a region of interest. Topography and optical intensity of emitted light are collected simultaneously. Fig. 3 shows a 2-dimensional (2D) image of topography of a  $30 \mu\text{m}$  long GaN/AlGaIn nanowire, a 2D image of the light intensity from the NSOM scan, and a 3-dimensional (3D) image combining the data from the 2D pictures. All data are plotted as a function of position in *x* and *y* over a  $10 \mu\text{m} \times 10 \mu\text{m}$  region.

In the measurement shown in Fig. 3, the SEM electron beam was held fixed at a point near the top of the image. The beam excitation condition was 20 kV with a probe current of  $3 \times 10^{-10}$  A. The diameter of the wire at the point of excitation was approximately 600 nm, based on SEM and AFM imaging. The near-circular luminescence that appears at the end of the GaN nanowire,  $\sim 6 \mu\text{m}$  from the point of excitation, is a result of waveguiding. Luminescence that is created when electron-hole pairs recombine is non-directional. For the minority diffusion length measurement, the NSOM collects the fraction that is emitted in the vertical direction. Much of the remaining light is

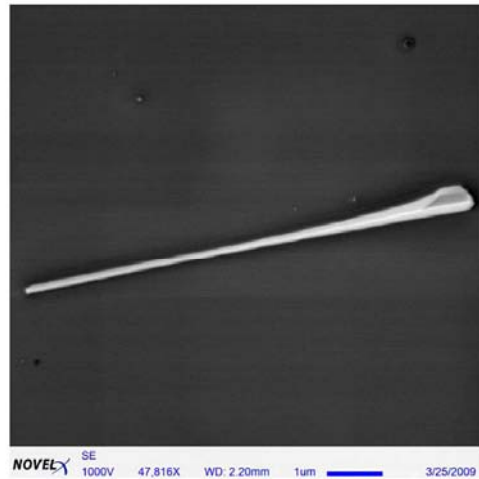


Fig. 2. SEM image (1 kV) of GaN/AlGaIn core-shell nanowire. Magnification is 47.816X.

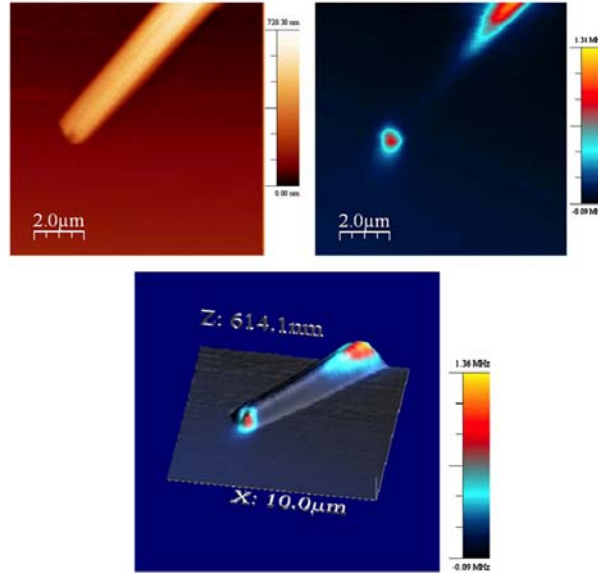


Fig. 3. Topography (top left), near-field luminescence (top right) image, and 3-D combination of topography and near-field luminescence from a GaN nanowire under point source excitation (bottom). The image dimensions are  $10 \mu\text{m} \times 10 \mu\text{m}$ . In the bottom image, the color variation corresponds to optical intensity variations, superimposed on a monochromatic topography image.

waveguided along the wire. Because of the relatively broad and strong defect-related CL emission, a majority of the light is below band gap and is not expected to cause significant reabsorption and the generation of new carriers (photon recycling).

For diffusion in one dimension, the minority carrier distribution and resulting luminescence distribution is given by

$$I = \frac{g}{2L} e^{(-x/L)}$$

where  $g$  is the generation rate and  $L$  the diffusion length. Diffusion lengths can be extracted from the inverse slope of the intensity distribution on a semi-logarithmic plot.

Fig. 4 shows the NSOM intensity as a function of distance from the point of excitation on the GaN nanowire in Fig. 3. The data show an oscillation caused by relative movement in the electron beam and sample while scanning which can produce a sinusoidal artefact in the raw data. This can be mitigated by analyzing the data in a logarithmic Fourier plot and removing the sinusoidal artefact. The diffusion length for this case was measured to be  $1.1 \pm 0.05 \mu\text{m}$ . This is within the relatively large range of minority hole carrier diffusion lengths reported for n-type thin films of GaN [10].

Measurements exist for majority carrier mobilities in both n-type and p-type GaN nanowires [7,11]. Extracting minority carrier mobility from the diffusion length measured here would require an independent lifetime measurement, generally done with time-resolved photoluminescence. However, the direct measure of  $L_d$  is often the relevant parameter for minority carrier devices.

Fig. 5 shows a series of measurements of the intensity distribution on a  $10\text{-}\mu\text{m}$ -long wire, measured for excitation at a single spot as a function of probe current. Using the lower probe

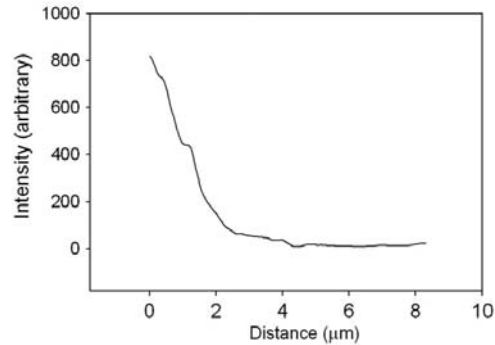


Fig. 4. Intensity as a function of distance resulting from minority carrier diffusion in 1D. GaN wire diameter is 500 nm. Excitation conditions were 20 keV and  $3 \times 10^{-10}$  A probe current.

currents of  $6 \times 10^{-12}$  and  $3 \times 10^{-11}$  A, extracted diffusion lengths of  $1.3 \pm 0.1 \mu\text{m}$  were consistent with results in Fig. 3. However, as the probe current was increased to  $1 \times 10^{-10}$  A, the extracted diffusion length increased to  $2.7 \mu\text{m}$ . When the probe current was increased again to  $6 \times 10^{-10}$  A, the extracted diffusion length increased further to  $3.1 \mu\text{m}$ .

In transport imaging in epitaxial layers, an increase in excitation intensity can begin to affect the minority carrier diffusion length measurement if one moves out of the low injection regime and into a regime where the recombination



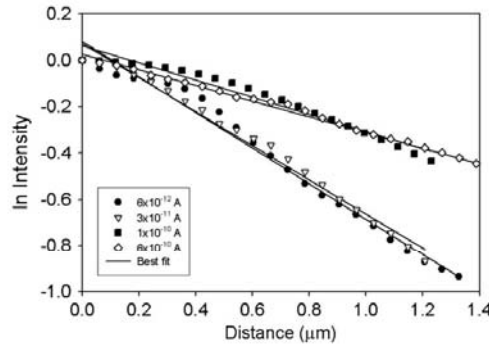


Fig. 5. Intensities as a function of distance. GaN wire diameter is 700 nm. Excitation conditions were 20 keV with varying probe currents ( $6 \times 10^{-12}$ ,  $3 \times 10^{-11}$ ,  $1 \times 10^{-10}$ , and  $6 \times 10^{-10}$  A).

lifetime becomes a function of the local excitation, due to the effect on the local majority carrier population. In this case, one normally observes a decrease in  $L_d$  at higher excitation. One assures operation in the low injection regime by measuring as a function of probe current until the measured value for  $L_d$  asymptotes to a constant value at the lower probe currents.

Results in Fig. 5 illustrate a related, though different challenge for the NSOM imaging measurements in proximity to an electron beam. The lower probe currents produce a consistent value for  $L_d$ . However once the probe current is raised above a certain value (which will change with each wire due to the dimensions and luminescent intensity), the diffusion length appears to increase as a function of the probe current. One explanation for this phenomenon is that higher probe currents result in higher intensity of scattered electrons from the incident beam. These electrons can interact with the NSOM fiber causing direct excitation of luminescence in the silica material. This can also be addressed by moving to lower excitation currents. In the future, this effect it can be further removed with the use of narrow band filters centered around the GaN band-edge luminescence at 3.4 eV ( $\sim 360$  nm), since the broad emission from the fiber is located

primarily in the 400–600 nm range. This assumes however that the nanowire luminescence is sufficiently intense to compensate for the loss in broadband signal.

In summary, we demonstrate a technique to provide direct imaging of minority carrier transport in a wide range of optically active materials. Transport imaging has been demonstrated for the first time in GaN nanowires, using a combination of scanning near-field microscopy and SEM. This technique provides both the optical sensitivity and the spatial resolution required to resolve a minority carrier diffusion length within a single nanowire. Initial measurements on the AlGaIn/GaN wires described here give a minority carrier diffusion length of  $1.2 \pm 0.2 \mu\text{m}$ .

#### Acknowledgements

This work was supported at the Naval Postgraduate School by National Science Foundation Grants DMR 0526330 and DMR 0804527. This research is also supported by DOE Basic Energy Sciences and Sandia's Laboratory Directed Research and Development program. Sandia is a multiprogram laboratory operated by Sandia Corporation, a Lockheed Martin Company, for the United States Department of Energy's National Nuclear Security Administration under Contract no. DE-AC04-94AI85000.

#### References

- [1] H. Morkoc, Handbook of Nitride Semiconductors and Devices, Materials Properties, Physics and Growth, Wiley, 2008.
- [2] George T. Wang, A. Alec Talin, Donald J. Werder, J. Randall Creighton, Elaine Lai, Richard J. Anderson, Ilke Arslan, Nanotechnology, Institute of Physics Publishing, 2006 pp. 5773–5780.
- [3] J.R. Haynes, W. Shockley, Phys. Rev. 81 (1951) 835.
- [4] N.M. Haegel, T.J. Mills, M. Talmadge, C. Scandrett, C.L. Frenzen, H. Yoon, C.M. Fetzer, R.R. King, J. Appl. Phys. 105 (2009) 023711.
- [5] D.R. Luber, F.M. Bradley, N.M. Haegel, M.C. Talmadge, M.P. Coleman, T.D. Boone, Appl. Phys. Lett. 88 (2006) 163509.
- [6] D.N. Davydov, K.B. Shelimov, T.L. Haslett, M. Moskorits, Appl. Phys. Lett. 75 (1999) 1796.
- [7] G.T. Wang, A.A. Talin, D.J. Werder, J.R. Creighton, E. Lai, R.J. Anderson, I. Arslan, Nanotechnology 17 (2006) 5773.
- [8] Q. Li, G.T. Wang, Appl. Phys. Lett. 93 (2008) 043119.
- [9] A.A. Talin, G.T. Wang, E. Lai, R.J. Anderson, Appl. Phys. Lett. 92 (2008) 093105.
- [10] Z.Z. Bantic, P.M. Bridger, E.C. Piquette, T.C. McGill, Solid State Electron. 44 (2000) 221.
- [11] Zhaohui Zhong, Fang Qian, Deli Wang, C.M. Lieber, Nano Lett. 3 (2003) 343.

## LIST OF REFERENCES

- [1] Wikipedia *History of the transistor*, [http://en.wikipedia.org/wiki/History\\_of\\_the\\_transistor](http://en.wikipedia.org/wiki/History_of_the_transistor). Information dated 16 November 2009.
- [2] D. Giessel, *Basic Transistor Physics*, [http://ffden-2.phys.uaf.edu/212\\_fall2003.web.dir/David\\_Giessel/gate.html](http://ffden-2.phys.uaf.edu/212_fall2003.web.dir/David_Giessel/gate.html). (accessed September 2009).
- [3] P.J. Pauzauskie, and P. Yang, *Nanowire Photonics*, **Materials Today**, Volume 9, number 10. 36–45, October 2006.
- [4] N. M. Haegel, J. D. Fabbi, and M.P. Coleman, *Direct transport imaging in planar structures*, Applied Physics Letters, **84**, 1329, 2004.
- [5] D.R. Lubber, F. M. Bradley, N. M. Haegel, M. C. Talmadge, M. P. Coleman, and T. D. Boone, *Image transport for the determination of minority carrier diffusion length*, Applied Physics Letters, **88**, 163509, 2006.
- [6] D. Hambling, *Nanotechnology goes to war*. The Guardian, Thursday, 05 March 2009.
- [7] O. Madelung, *Semiconductors: Data Handbook*, 3rd edition. Springer-Verlag Berlin Heidelberg New York, ISBN: **3-540-40488-0**.
- [8] J.B. Schlager, K.A. Bertness, P.T. Blanchard, L.H. Robins, A. Roshko, and N.A. Sanford, *Steady-state and time-resolved photoluminescence from relaxed and strained GaN nanowires grown by catalyst-free molecular-beam epitaxy*. Journal of Applied Physics, **103**, 124309 (2008).
- [9] C.H. Low, *Near Field Scanning Optical Microscopy (NSOM) of nano devices* Master's thesis, Naval Postgraduate School, Monterey, CA, December 2008.
- [10] Z.Z. Bandic, P.M. Bridger, E.C. Piquette, and T.C. McGill, *The values of minority carrier diffusion lengths and lifetimes in GaN and their implication for bipolar devices*, Solid-State Electronics, **44**, 221–228, (2000).
- [11] N. M. Haegel, T. J. Mills, M. Talmadge, C. Scandrett, C. L. Frenzen, H. Yoon, C. M. Fetzer, and R. R. King, *Direct imaging of anisotropic minority-carrier diffusion in ordered GaInP*, Journal of Applied Physics, **105**, 023711 (2009).
- [12] L. Novotny, *The History of Near-field Optics*, The Institute of Optics, University of Rochester, Rochester, NY. (2008).



- [13] G. W. Bryant and A.Liu, *Near-field scanning optical microscopy imaging: theory, simulation and experiment*, National Institute of Standards and Technology, Gaithersburg, MD (1999).
- [14] F.J. Giessibl and C.F. Quate, *Exploring the nanoworld with atomic force microscopy*, Physics Today, pg 44, December (2006).
- [15] N.M. Haegel, et al., *Transport Imaging with Near-Field Scanning Optical Microscopy*. Proc. of SPIE Vol. **7378**, **73782B** © 2009 SPIE.
- [16] S.D. Winchell, *Transport Imaging for the Study of Nanowires and Related Nanostructures*, Thesis, Naval Postgraduate School, Monterey, CA, June 2006.
- [17] University of Nebraska – Lincoln, <http://www.unl.edu/CMRAcfem/em.htm>, November 2009.
- [18] "MultiView 2000," Nanonics Imaging LTD <<http://www.nanonics.co.il/multiview-2000.html>> .
- [19] I. Horcas, R. Fernandez, J.M. Gomez-Rodriguez, J. Colchero, J. Gomez-Herrero, and A.M. Baro, Review of Scientific Instruments **78**, **013705** (2007).
- [20] B. Monemar, *III-V nitrides-important future electronic materias*. Journal of Material Science: Materials in Electronics **10** (1999) 227–254.
- [21] G.T Wang, A.A. Talin, D. J Werder, J.R. Creighton, E. Lai, R.J. Anderson, and I. Arslan, *Highly aligned, template-free growth and characterization of vertical GaN nanowires on sapphire by metal–organic chemical vapour deposition* Nanotechnology **17** (2006) **5773–5780**.
- [22] A.A. Talin, *Growth, luminescence and transport in GaN nanowires*. Power point presentation given at NPS September 2008.
- [23] R.S. Quimby, *Photonics and lasers, an introduction*. John Wiley and Sons. Copyright 2006.
- [24] L. Baird, et al., Imaging, *Minority carrier diffusion in GaN nanowires using near field optical microscopy* Physica B **404** (2009) 4933–4936.
- [25] C.P. Ong *Measurement of Minority Charge Carrier Diffusion Length in Gallium Nitride Nanowires using Electron Beam Induced Current (EBIC)* Thesis, Naval Postgraduate School, Monterey, CA, December 2009.
- [26] M.-K. Seo, J.-K. Yang, K.-Y. Jeong, H.-G. Park, F. Qian, H.-S. Ee, Y.-S. No, and Y.-H. Lee, *Modal Characteristics in a Single-Nanowire Cavity with a Triangular Cross Section* Nano Lett, 2008, **8** (12), 4534–4538.

## INITIAL DISTRIBUTION LIST

1. Defense Technical Information Center  
Ft. Belvoir, Virginia
2. Dudley Knox Library  
Naval Postgraduate School  
Monterey, California
3. Professor Andres Larraza  
Chairman, Department of Physics  
Naval Postgraduate School  
Monterey, California
4. Professor Nancy M. Haegel  
Naval Postgraduate School  
Monterey, California
5. Lee Baird  
Naval Postgraduate School  
Monterey, California
6. Alec Talin  
Sandia National Laboratories  
Livermore, California
7. George Wang  
Sandia National Laboratories  
Albuquerque, New Mexico